International Journal of Biological Macromolecules 222 (2022) 2452–2466

Contents lists available at ScienceDirect

International Journal of Biological Macromolecules

journal homepage: www.elsevier.com/locate/ijbiomac

The immobilization protocol greatly alters the effects of metal phosphate modification on the activity/stability of immobilized lipases

José R. Guimarães [a,b], Diego Carballares [a], Javier Rocha-Martin [c], Paulo W. Tardioli [b,*], Roberto Fernandez-Lafuente [a,d,**]

[a] Departamento de Biocatálisis, ICP-CSIC, Campus UAM-CSIC, 28049 Madrid, Spain
[b] Graduate Program in Chemical Engineering (PPGEQ), Laboratory of Enzyme Technologies (LabEnz), Department of Chemical Engineering, Federal University of São Carlos (DEQ/UFSCar), Rod. Washington Luís, km 235, 13565-905 São Carlos, SP, Brazil
[c] Department of Biochemistry and Molecular Biology, Faculty of Biology, Complutense University of Madrid, José Antonio Novais 12, Madrid 28040, Spain
[d] Center of Excellence in Bionanoscience Research, Member of the External Scientific Advisory Board, King Abdulaziz University, 21589 Jeddah, Saudi Arabia

ARTICLE INFO

Keywords:
Solid-phase enzyme mineralization
Enzyme stabilization
Tuning enzyme specificity

ABSTRACT

Mineralization of immobilized enzymes has showed to couple the advantages of both processes. Here, the influence of the immobilization protocol on the effects of mineralization has been investigated. The lipases from *Thermomyces lanuginosus* and *Candida rugosa* were immobilized on octyl-, vinyl sulfone (VS) octyl (blocked with different nucleophiles) and glutaraldehyde- (at different pH values) agarose beads. The stability, activity and specificity of the biocatalysts were very different, both the differently blocked VS-biocatalysts and the glutaraldehyde biocatalysts prepared at different pH. All biocatalysts were submitted to mineralization using different metals. The activity, specificity and stability effects of the mineralization strongly depended on the enzyme and on the immobilization protocol. For the same enzyme, a mineralization protocol could be negative, positive or present no effect depending on the enzyme immobilization procedure and substrate. In the best cases, activity could be increased by a two-fold factor, while stability was significantly improved in many instances. These results highlight the great potential of mineralization of immobilized enzymes to improve their properties, as well as the great interactions that immobilization protocol and mineralization can exhibit. The combination of both methodologies greatly increases the possibilities to find a biocatalyst that can be suitable for a specific process.

1. Introduction

Lipases have been utilized in many different reactions because they present a broad specificity, are stable and active in a wide range of conditions and reaction media and can catalyze many different reactions [1–9] (including promiscuous ones) [10–12]. That way, they can be useful in very different applications [13–19]. Unfortunately, in many instances, the properties of lipases (as other enzymes) do not fit the requirements of an industrial catalyst, and their catalytic performance in industrial reactions (in many instances using substrates and conditions far from the physiological ones) is inadequate [20]. Nowadays, there are many strategies to solve some of the problems of lipases, their properties may be improved using metagenomics (to use the most adequate available enzyme) [21–24], site-directed mutagenesis [25–29] or directed evolution [30–33]. Another problem of enzymes is their water solubility, which can complicate their recovery. This makes their reuse and reaction control complex. Enzyme immobilization was the answer to solve this enzymes drawback, and nowadays it has been revealed as a tool to greatly improve many enzyme features, such as stability, selectivity, specificity, inhibition, etc. [34–45]. It can be also coupled with enzyme purification [46]. However, these benefits may be reached only if the immobilization protocol is carefully designed [47].

The lipase catalytic mechanism (interfacial activation) [3,48–50] causes their active center to be very flexible, and that way, lipase features are especially easy to be tuned by any of the previously described strategies, increasing the prospects of getting biocatalysts adequate for a

* Corresponding author at: Graduate Program in Chemical Engineering (PPGEQ), Laboratory of Enzyme Technologies (LabEnz), Department of Chemical Engineering, Federal University of São Carlos (DEQ/UFSCar), Rod. Washington Luís, km 235, 13565-905 São Carlos, SP, Brazil
** Correspondence to: R. Fernandez-Lafuente, Departamento de Biocatálisis, ICP-CSIC, Campus UAM-CSIC, 28049 Madrid, Spain.
E-mail addresses: pwtardioli@ufscar.br (P.W. Tardioli), rfl@icp.csic.es (R. Fernandez-Lafuente).

https://doi.org/10.1016/j.ijbiomac.2022.10.030
Received 18 July 2022; Received in revised form 3 October 2022; Accepted 5 October 2022
Available online 8 October 2022

specific process [51–56].

Among the lipase immobilization processes, the preparation of enzyme/metal salts nanoflowers has been established as a strategy that can give heterogeneous lipase biocatalysts and, at the same time, improve enzyme activity and stability in certain cases [57–61]. This strategy is based on the function of some residues of the enzyme surface as crystal nucleation points, generating crystal structures that have the appearance of the petals of a flower, or even of the whole flower (hence the name) after full growth. Although bearing an undeniable interest, the poor mechanical resistance of these nanoflowers is delaying their implementation. To solve this problem, the trapping of the enzyme nanoflower in structures bearing better mechanical resistance has been proposed, together with the use of magnetic materials to facilitate their handling [62–69].

Our research group recently proposed performing the modification by metal phosphate on already immobilized enzymes as an alternative to solve the nanoflowers fragility while maintaining some of the mineralization benefits [70]. If the enzyme mineralization was performed on previously immobilized enzymes, the researcher can select the support based on its mechanical resistance (and reap the benefits achieved during enzyme immobilization), avoiding the difficulties derived from the management of the small and fragile nanoflowers. Moreover, the mineralization of immobilized enzyme couples the positive effects of enzyme mineralization during nanoflowers production with the benefits of enzyme immobilization in preexisting solids [70]. In this first report, several enzymes were immobilized on octyl agarose beads via interfacial activation [71] and modified with diverse metal phosphates. It was found that the effects of the metal phosphate modification were clearer and more positive using highly loaded biocatalyst, suggesting that enzyme crowding could facilitate some of the positive effects of enzyme mineralization [70]. The effects depended on the nature of both enzyme and metal, in some instances enabling very significant stabilizations, and optimal results were achieved using the metal phosphate in the modification of already immobilized enzymes. The incubation with only sodium phosphate or only metal chloride, as well as the immobilization on previously modified supports (the supports could be modified by using metal phosphates) which produced significantly reduced effects [70]. This modification of the support complicates finding any structural proof of the reasons for the great modification of the enzyme properties upon mineralization. However, the important alteration of the functional properties of the enzymes after their mineralization presented a significant interest. The study was later extended to the use of diverse commercial biocatalysts [72]. The immobilized enzyme mineralization cannot produce a tridimensional nanoflower, as the enzymes will be located on a flat planar surface, but the previous results suggest that the positive effects of the building of nanoflowers may be, at least partially, achieved using this solid-phase strategy. However, we cannot talk of nanoflowers, as these tridimensional structures will never be achieved.

There are some reports showing that the immobilization protocol can greatly alter the effect of some chemical or physical modifications of immobilized enzymes [73–77]. The mineralization of the commercial lipase biocatalysts offered very different results to those described using the octyl-lipases, suggesting that this could be the case for enzyme mineralization [72].

In a very recent paper [78], the authors have shown that the nucleation induced by a protein during the production of metal–organic frameworks produced using 2-methylimidazole and zinc acetate strongly depended on the tridimensional structure of the protein, origin salt crystals with very different structures.

In this new communication, we have studied the possible influence of the immobilization protocol on the effects that the metallization of the immobilized lipases can present. For this reason, we will compare the results obtained when modifying with metal phosphate enzymes immobilized using octyl agarose [71,79] with other two immobilization techniques whose versatility permits to tailor the immobilized enzyme features.

The first one is the immobilization of the lipases on amino-glutaraldehyde agarose beads [80]. The main immobilization cause on these supports is the ionic exchange of the enzyme on the support surface, followed by the establishment of some covalent bonds between the primary amino bonds of the adsorbed enzyme and the glutaraldehyde groups in the support [81–83]. As it has been reported that the pH in the immobilization process greatly affects the enzyme features after its immobilization, we performed the immobilization at pH 5 and 8 [84–89] (Fig. 1).

The second one is the immobilization of the lipases on agarose beads simultaneously presenting octyl and vinyl sulfone groups, an immobilization protocol that produces some of the most stable formulations described in the literature for the employed enzymes [90]. In this case, the enzyme is first immobilized via interfacial activation, and after changing the conditions, some groups of the enzyme (e.g., Lys, His, Cys, Tyr) [91] can react with the vinyl sulfone groups [90]. This strategy has a final step that requires the blocking of the remaining reactive groups of the support with a nucleophile. This step enables tailoring of the enzyme-support interactions by using reagents with very different physical properties [90,92–95] (Fig. 2). Moreover, it greatly alters the functionality of the enzymes (enzyme stability and activity) and this has been correlated to the promotion of different enzyme structures [96]. Furthermore, it has been shown how the different enzyme-support interactions promote different inactivation pathways [96], similarly to the enzyme rigidification of different enzyme areas [97]. That way, playing with the blocking reagent, we will have an immobilized enzyme collection with exactly the same enzyme distribution in the support particle, orientation with respect to the support surface (they are interfacially activated) and number of enzyme support bonds, but bearing a different structure and functional properties.

Both immobilization strategies will permit to analyze if the enzyme structure or orientation regarding the support (or both) may alter the effects of the mineralization as it has been found for other modifications. As model enzymes to analyze these possible immobilization protocol/mineralization interactions, we have selected the two enzymes that were more significantly stabilized by mineralization when using octyl agarose [70], both very popular ones: the lipases from *Thermomyces lanuginosus* [98] and from *Candida rugosa* [99–102]. The use of at least two different enzymes permitted to get more generalized conclusions.

2. Materials and methods

2.1. Materials

A TLL formulation with 20.77 mg protein/mL (kindly donated by Novozymes Spain (Madrid, Spain)) was utilized in this paper. Lipase from *Candida rugosa* (CRL) was acquired from Sigma-Aldrich (St. Louis, MO, USA), it was a solid powder with 3.12 mg protein/g of powder. Bradford's reagent (utilized to calculate the protein concentration [103]), *p*-nitrophenyl-butyrate (*p*-NPB), triacetin, *R*- and *S*-methyl mandelate, acetonitrile for HPLC (gradient grade, ≥99.9 %), glycine, aspartic acid, ethylenediamine (EDA), cysteine, Tris(2-aminoethyl) amine (TrisAEA), glutaraldehyde (GA) solution (25 % in H_2O), $CoCl_2$, $CuCl_2$ and $ZnCl_2$ were purchased from Sigma-Aldrich (St. Louis, MO, USA). Divinyl-sulfone (DVS) was purchased from Thermo Fisher Scientific Spain (Madrid, Spain). Octyl Sepharose® CL-6B was acquired from GE Healthcare (Uppsala, Sweden). All other reagents were of analytical grade.

2.2. Methods

All experiments were performed at least by triplicate, and the values are presented as mean values and standard deviation. Protein concentration was determined using Bradford method [103].

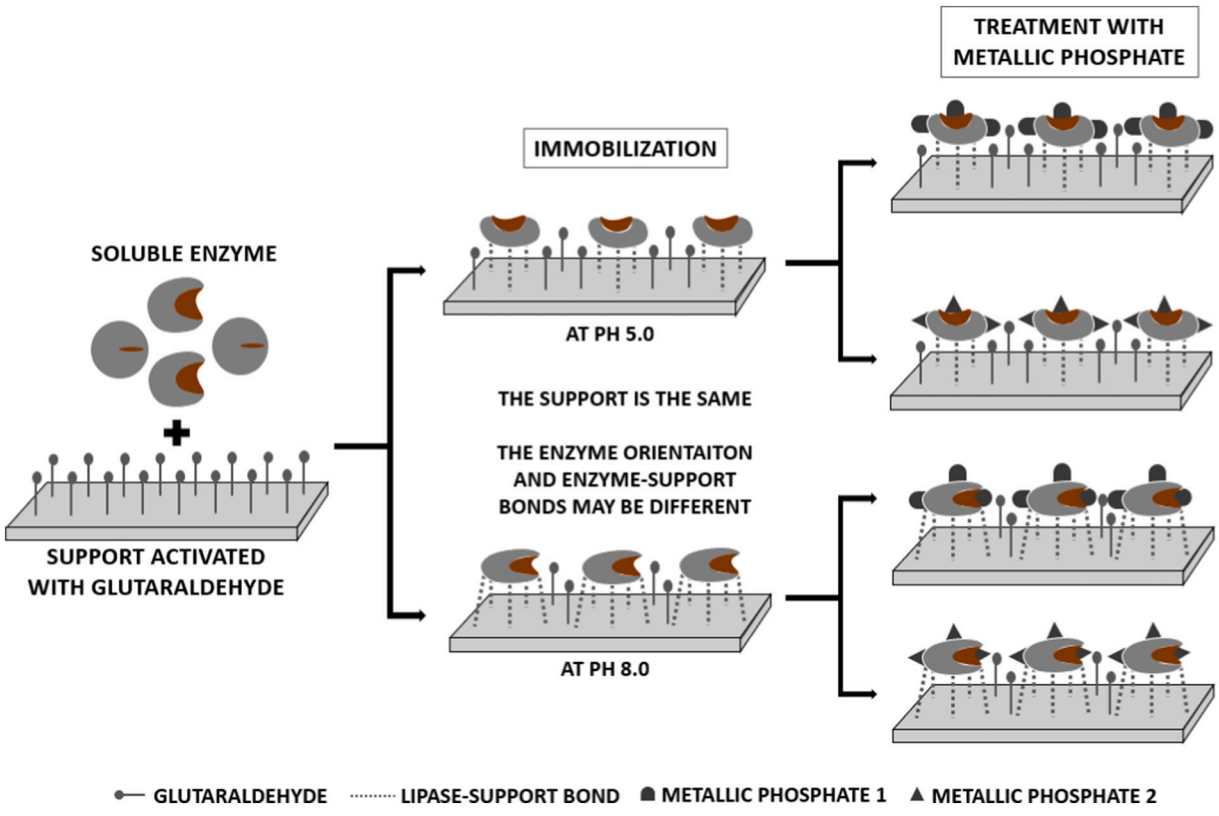

Fig. 1. Schematic representation of enzyme immobilization on glutaraldehyde-activated support at different pH values.

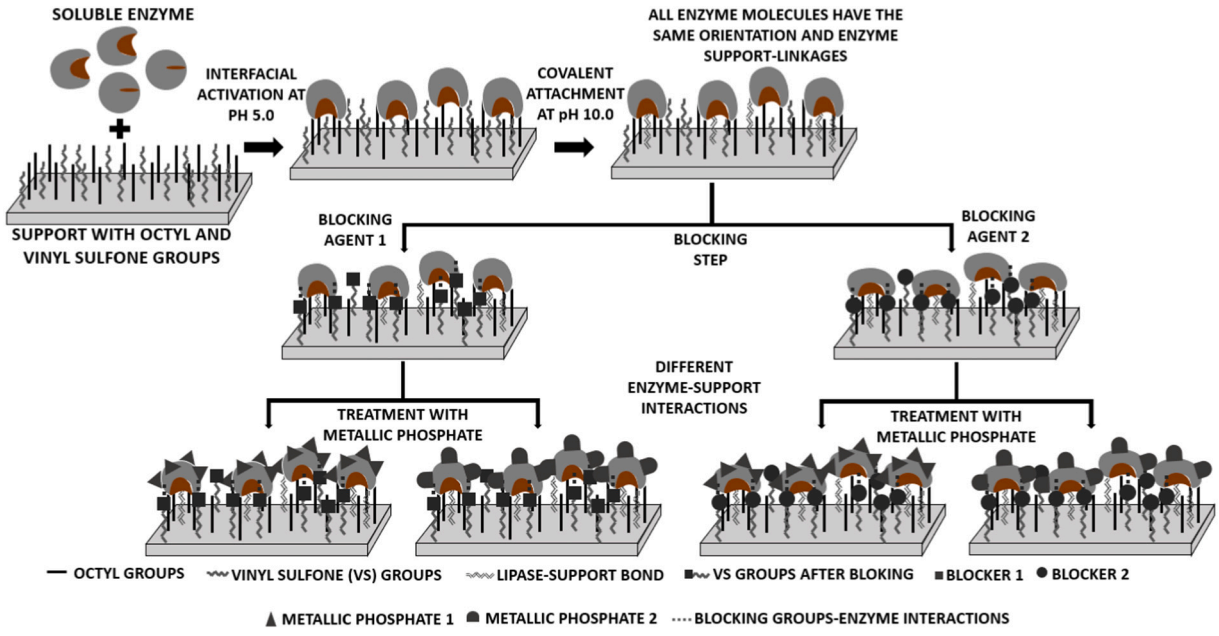

Fig. 2. Schematic representation of enzyme immobilization on octyl and divinyl sulfone groups heterofunctionalized support.

2.2.1. Preparation of octyl-vinyl sulfone agarose beads

The octyl-vinyl sulfone agarose support was prepared following the methodology described by Albuquerque et al. [90]. 1 g of octyl agarose was added to 20 mL of 350 mM divinyl-sulfone prepared in 333 mM sodium carbonate at pH 11.5, having a vinyl sulfone group in the support. Activation of the support was carried out at room temperature under gentle stirring for 2 h. Afterwards the support was vacuum filtered, washed 5 folds with 20 volumes of distilled water and stored at 4–6 °C.

2.2.2. Preparation of the glutaraldehyde-agarose support

A mass of 1 g of amine agarose (prepared according to the methodology described by Fernandez-Lafuente et al. [104]) was added to 10 mL of 10 % glutaraldehyde prepared in 200 mM sodium phosphate at pH 7. The activation process took place at room temperature under gentle stirring for 16 h. Then, the support was vacuum filtered, washed 5 times

with 20 volumes of distilled water and stored at 4–6 °C.

2.2.3. Immobilization of lipases

In all cases, activity immobilization yield (percentage of offered enzyme activity that is immobilized on the support) and expressed activity (percentage of observed activity with respect to the expected one from the immobilization yield) are utilized to define the immobilizations [105]. The mineralization only affects the expressed activities. The enzyme load is calculated from the offered activity and the enzyme activity that remains in the supernatant. Activity is not released from the support during the washings, but around 100 mg of support is lost in the filters during the washing steps (this is a problem in the lab that may not occur using other washing devices). In fact, the covalent immobilizations makes that not protein bands may be detected in SDS-PAGE experiment (not shown results) [90].

2.2.3.1. Immobilization of lipases on octyl-agarose beads. A mass of 10 g of support was added to 100 mL of enzyme solution prepared in 5 mM sodium phosphate at pH 7.0 (enzyme loads: TLL: 20 mg/g and CRL: 30 mg/g). The immobilization was conducted at room temperature under gentle stirring for 2 h (Agimatic-S (JP Selecta) (Barcelona, Spain)). The enzyme activity in the supernatant, suspension and a reference (where octyl agarose was substituted by inert agarose) were quantified using *p*-NPB assay throughout the immobilization course. Then, the suspensions were filtered and the biocatalysts were washed 5 folds with 20 volumes of distilled water, and stored at 4–6 °C.

2.2.3.2. Immobilization of lipases on octyl-vinyl sulfone agarose beads. A mass of 10 g of support was added to 100 mL of enzyme solution prepared in 5 mM sodium acetate at pH 5.0 (enzyme loads: TLL: 20 mg/g and CRL: 30 mg/g) [90]. In this step, pH 5.0 was used to favor interfacial activation as the main cause for enzyme immobilization [90]. The immobilization was conducted at room temperature under gentle stirring for 2 h (Agimatic-S (JP Selecta) (Barcelona, Spain)). The enzyme activity in the supernatant, suspension and a reference were quantified using *p*-NPB assay throughout the immobilization course. Then, the biocatalysts were vacuum filtered, washed 5 times with 20 volumes of distilled water, and recovered. The biocatalysts were resuspended in 100 mM sodium carbonate at pH 10.0 in a biocatalyst/buffer ratio of 1/10 (w/v). This step was used to favor the formation of the enzyme-support covalent bond(s). The reaction was conducted at room temperature for 24 h. Afterwards, the biocatalysts were vacuum filtered and recovered. Finally, 1 g of biocatalyst was added to 10 mL of 2 M blocking agent (glycine, aspartic acid, cysteine, EDA, TrisAEA) at pH 10.0. This step was carried out at room temperature under gentle stirring for 48 h in order to modify the residual vinyl sulfone moieties. Then, the biocatalysts were vacuum filtered, washed 10 folds with 20 volumes of distilled water, and stored at 4–6 °C.

2.2.3.3. Immobilization of lipases on amino-glutaraldehyde (Glu)-agarose beads. A mass of 10 g of support was added to 100 mL of enzyme solution prepared in 5 mM sodium phosphate at pH 7.0 (enzyme loads: TLL: 20 mg/g and CRL: 30 mg/g). The immobilization was conducted at room temperature under gentle stirring for 2 h (Agimatic-S (JP Selecta) (Barcelona, Spain)). The immobilization was followed measuring *p*-NPB activity of the supernatant, suspension and reference solutions. After immobilization, the biocatalysts were filtered, washed 5 folds with 20 volumes of distilled water, vacuum dried and stored at 4–6 °C by a minimum of 48 h before any use.

2.2.4. Modification of immobilized enzyme with metallic salt/phosphate

The immobilized enzymes were modified with metallic salt/phosphate following the methodology described by Guimarães et al. for octyl agarose immobilized lipases [70]. 1 g of immobilized enzyme was suspended in 10 mL of 10 mM sodium phosphate/125 mM NaCl at pH 7.4 and, then, 400 μL of 230 mM of the corresponding metallic salt solution was added. The enzyme treatment was conducted at room temperature under gentle stirring for 5 h (Agimatic-S (JP Selecta) (Barcelona, Spain)). After modification, the suspension was filtered and the biocatalysts were washed 5 folds with 20 volumes of distilled water, and stored at 4 °C.

2.2.5. Thermal inactivations of the different lipase preparations

In a standard experiment, 1 g of immobilized biocatalyst was suspended in 10 mL of 10 mM Tris-HCl at pH 7.0 and incubated at different temperatures (immobilized TLL: 75 °C and immobilized CRL: 70 °C). Periodically, samples of 50 μL of the inactivation suspensions were collected to determine their residual activities (current activity divided by the initial one in percentage). The experiments were performed employing *p*-NPB as substrate.

2.2.6. Enzyme activity assays

One unit of activity (U) was defined as the amount of enzyme that hydrolyzes one μmol of substrate per minute under the described conditions.

2.2.6.1. Hydrolysis of p-NPB. A volume of 50 μL of 50 mM *p*-NPB dissolved in acetonitrile was added into a mixture of 2.5 mL of 25 mM sodium phosphate at pH 7.0. The experiments were performed in a Jasco V-730 spectrum (Madrid, Spain) with a stirring system and temperature regulation. To initialize the reaction, a volume of 50 μL of enzyme solution or immobilized enzyme suspension was added. The reaction was carried out at room temperature under magnetic stirring. The quantification of hydrolytic activity was determined by the increase in absorbance at 348 nm produced by the release of p-nitrophenol (*p*-NP) (isosbestic point of *p*-NP, its ε under these conditions is 5150 M^{-1} cm^{-1}) for 300 s [106].

2.2.6.2. Hydrolysis of triacetin. 125 mg of immobilized enzyme were added to 10 mL of 50 mM of triacetin prepared in 50 mM of sodium phosphate at pH 7.0. Hydrolysis was carried out at room temperature under gentle stirring (Agimatic-S (JP Selecta) (Barcelona, Spain)), and quantified by detection of 1,2 and 1,3 diacetin (under these conditions, the produced 1,2 diacetin suffers acyl migration giving 1,3 diacetin) [107]. The degree of conversion (two points over 5 % and under 25 %, to ensure linearity and minimize experimental error caused by the initial acid content of the samples) was calculated by HPLC in a Waters 486 chromatograph (Waters, Millford, USA) equipped with a UV/VIS detector (set to 230 nm) using a Kromasil C18 column (15 cm × 0.46 cm) with a mobile phase composed of 85 % (*v*/v) of water and 15 % (v/v) of acetonitrile with a flow rate of 1 mL/min. The retention times were 4 min for 1,2 and 1,3 diacetins (under these conditions. They eluted at the same retention time) and 18 min for triacetin [108].

2.2.6.3. Hydrolysis of R- or S-methyl mandelate. 250 mg of immobilized lipase were added to 10 mL of 50 mM *R*- or *S*-methyl mandelate in 50 mM sodium phosphate solution at pH 7.0. Hydrolysis was carried out at room temperature under gentle stirring (Agimatic-S (JP Selecta) (Barcelona, Spain)), and the substrate and product concentrations were determined by HPLC using a Waters 486 chromatograph (Waters, Millford, USA). The equipment features a UV/VIS detector (set to 230 nm) and a Kromasil C18 column (15 cm × 0.46 cm). The mobile phase was 10 mM ammonium acetate and acetonitrile (65 %–35 % (v/v)) at pH 2.8 with a flow rate of 1 mL/min. The retention times were 2.5 min for mandelic acid and 4.2 min for the *R*- or *S*-methyl mandelate. Conversions under 25 % (two points over 5 % and under 25 %, to ensure linearity and minimize experimental error caused by the initial acid content of the samples) were used to calculate enzyme activity [94]. Activities ratio was defined as the activity versus the *R*-isomer/activity versus the *S*-isomer. This reaction was utilized to check the operational

stability of the biocatalysts. For this purpose, a syringe with a silica filter at the bottom to prevent the leakage of the biocatalyst was used, utilizing 1 g of biocatalysts and 10 mL of 10 mM ester solution in 200 mM sodium phosphate at pH 7 for 2 h. After each cycle, the biocatalysts were washed 3 times 10 mL with distilled water before reloading the substrate solution. Activity was determined when <20 % of the ester had been hydrolyzed.

3. Results and discussion

3.1. The case of TLL biocatalysts

3.1.1. Immobilization of TLL in the different supports

First, TLL and CRL have been immobilized on octyl-, octyl-VS and amino-glutaraldehyde-agarose beads. Our objective was to fully coat the support surface with enzyme molecules, as this was found to favor the effects of the mineralization on the enzyme properties [70]. That way, in all cases, we utilized an excess of enzyme on the immobilization. Fig. 1S shows the immobilization course of TLL on octyl agarose. Around 10 mg of enzyme extract/g of support are immobilized (50 % of the offered activity). Using octyl-VS agarose beads (Fig. 2S), the immobilization rate and yield are very similar. The immobilization of the enzyme on glutaraldehyde was performed at pH 5 and 8 (Fig. 3S). Immobilization was almost total in both cases.

Table 1 summarizes the activity of the different TLL preparations versus *p*-NPB, triacetin and *R*- and *S*-methyl mandelate. Starting with TLL-octyl, maximum activity is observed using *p*-NPB, being the activity versus triacetin >10 folds lower. The activity versus mandelate esters is around 100 fold lower than versus triacetin, preferring the hydrolysis of the *R*-isomer by almost a 2 fold factor.

Analyzing the VS-octyl biocatalysts, clear differences may be found among the different biocatalysts as a function of the blocking agent utilized as reaction end point. The Gly blocked biocatalysts presented over 2.3 more activity versus *p*-NPB than the octyl preparation, while their activity decreased by <10 % the activity of this biocatalyst versus triacetin. In the mandelate esters, the activity was almost maintained using the *R*-isomer, while it decreased using the *S*-isomer. That way the activities ratio versus both isomers became 3. If the blocking is performed using EDA, activity versus *p*-NPB is slightly lower than in the other case, while the decrease in the activity versus triacetin was more significant (to around 75 % of that of the octyl preparation). Regarding the methyl mandelate isomers, the activity versus the *R*-isomer slightly increased while the activity versus the *S*-isomer decreased compared to the octyl preparation, the activities ratio became almost 5. Using TrisEAE as blocking agent, the activity versus *p*-NPB was similar to the case of EDA, higher using triacetin, and the clearest difference is using the mandelic esters. The activity versus the *R*-isomer decreased while the activity versus the *S*-isomer was maintained (compared to the TLL octyl biocatalyst), the resulting activities ratio is lower than 1. Using Asp to block the biocatalyst, activity versus *p*-NPB was 2.2 fold higher than using the octyl preparation, the activity was 85 % using triacetin and decreased more versus the *R*- than versus the *S*-methyl mandelate, the activities ratio become 1.25. Blocking using Cys gave an activity doubling that of the TLL-octyl preparation versus *p*-NPB, maintaining 60 % of the activity versus triacetin, and decreased the activity more versus *S*-methyl mandelate than versus the *R*-isomer, giving an activities ratio of 2.5. That way, the functional properties of all the biocatalysts were quite different depending on the blocking agent, as it has been previously reported [90,92–94] altering in a very significant way the enzyme specificity and enantiospecificity. Considering that all biocatalysts have the same enzyme distribution on the support, the same orientation (the enzyme is interfacially activated) and the same number of enzyme-supports bonds, the differences should be related to the only difference among the biocatalysts: the different support surface moieties. That way, the different interactions between enzyme and support surface should be the reason for these different enzyme features. Comparing the vinyl sulfone- octyl biocatalysts to the octyl biocatalyst, differences are extended to possible distortions caused on the enzyme surface by the covalent bonds. Some role of the immobilization pH cannot be discarded, as it has been reported to alter also the functional properties of lipases immobilized on hydrophobic supports, being also associated to the creation of different enzyme structures [96]. In any case, the objective of having a collection of biocatalysts with very different functional properties has been accomplished.

Using the glutaraldehyde preparations, again great differences could be found depending on the immobilization pH value. The activity versus *p*-NPB of the enzyme immobilized at pH 8 is 2.5 fold lower than that of the enzyme immobilized at pH 5. Although the support enzyme loading is double than that when using the octyl preparation (because we use agarose 6BCL and immobilization yields is next to 100 % (Fig. 3S)), the activity versus *p*-NPB is much lower than those described for the hydrophobic supports (near 100 fold in the most extreme case). Using triacetin, activity is again much lower than in the other biocatalysts (by almost a factor of 50), but the activities of both glutaraldehyde biocatalysts becomes more similar (1.35 fold higher for the enzyme immobilized at pH 5). However, the activity versus the methyl mandelate isomers is much higher than that found for the octyl biocatalysts (by almost 7 fold). In fact, the glutaraldehyde TLL biocatalysts presented more activity versus methyl mandelate than versus triacetin, in

Table 1
Mass activity (immobilized biocatalyst) of different TLL biocatalysts with different substrates: 50 mM *R*- or *S*-methyl mandelate (pH 7 and 25 °C), 50 mM of triacetin (pH 7 and 25 °C) and 1 mM of *p*-NPB (pH 7 and 25 °C). Experiments were performed as described in methods.

Biocatalyst	Activity (U/g)			
	p-NPB	Triacetin	*R*-Mandelate	*S*-Mandelate
TLL-octyl	1390.9 ± 25.0	110.9 ± 5.4	1.3 ± 0.06	0.7 ± 0.03
Gly-TLL-VS-octyl	3279.0 ± 20.6	102.1 ± 4.1	1.2 ± 0.05	0.4 ± 0.02
EDA-TLL-VS-octyl	3038.8 ± 51.7	83.6 ± 3.7	1.4 ± 0.02	0.3 ± 0.01
TrisAEA-TLL-VS-octyl	3000.6 ± 28.3	94.0 ± 4.9	0.6 ± 0.02	0.07 ± 0.003
Asp-TLL-VS-octyl	3109.6 ± 132.4	94.0 ± 3.7	0.5 ± 0.02	0.4 ± 0.02
Cys-TLL-VS-octyl	2755.4 ± 98.1	64.1 ± 2.2	0.5 ± 0.02	0.2 ± 0.01
TLL-Glu (pH 5.0)	37.6 ± 2.2	2.7 ± 0.1	10.6 ± 0.5	10.6 ± 0.5
TLL-Glu (pH 8.0)	15.6 ± 0.1	2.0 ± 0.1	9.1 ± 0.4	13.8 ± 0.7

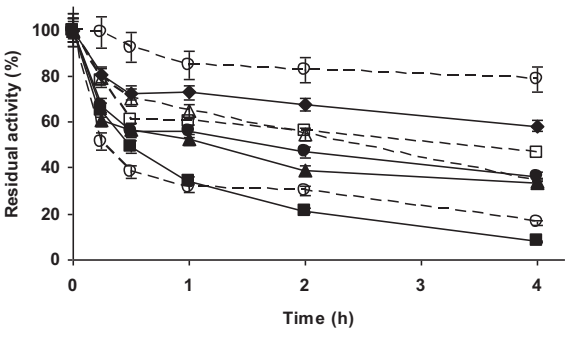

Fig. 3. Inactivation courses of different TLL biocatalysts in 10 mM Tris-HCl buffer at pH 7.0 and 75 °C. Other specifications are described in Methods. TLL-octyl (solid square and solid line); Gly-TLL-VS-octyl (solid rhombus and solid line); EDA-TLL-VS-ocyl (solid circles and solid line); TrisAEA-TLL-VS-octyl (solid triangles and solid line); Asp-TLL-VS-octyl (open squares and dotted line); Cys-TLL-VS-octyl (open rhombus and dotted line); TLL-Glu (pH 5.0) (open circles and dotted line); TLL-Glu (pH 8.0) (open triangles and dotted line).

opposition with the other preparations. The enzyme immobilized at pH 5 did not discriminate between both isomers, while the enzyme immobilized at pH 8 preferred the *S*-isomer (with an activities ratio of around 0.65), as opposed to most of the octyl preparations. That way, all the TLL biocatalysts have fully different specificities, in agreement with previous reports [74,82].

Another functional feature that is modulated by the immobilization protocol and blocking step is the stability of the immobilized enzyme [84,86,87,89,90,92–94]. Fig. 3 shows the inactivation courses of all the prepared biocatalysts. TLL-octyl presented a stability similar to that of the enzyme immobilized at pH 5 on glutaraldehyde, while the enzyme immobilized at pH 8 on glutaraldehyde was more stable. It should be considered that TLL has been immobilized in absence of detergent, that way, very likely, both glutaraldehyde biocatalysts may have mainly lipase dimers, with the open form of one molecule of TLL stabilized by another open lipase [109–112]. Furthermore, at pH 8, the possibilities of having a more intense multipoint covalent attachment increased, explaining the higher stability of this biocatalyst [42]. As previously reported [90,96], all the octyl-VS biocatalyst improved the stability compared to the octyl biocatalyst, but there are clear differences between them. The most stable biocatalyst is that blocked with Cys, followed by the biocatalyst blocked using Gly (both clearly more stable than the enzyme immobilized on glutaraldehyde at pH 8), while the biocatalyst blocked with EDA and TrisEAE gave the lowest stabilities among these biocatalysts. That way, also the stability of the different biocatalysts differed, for both glutaraldehyde and VS-octyl ones, confirming that the enzyme presented very different functional features, our initial objective. Next, we have submitted the different biocatalysts to the incubation with metal phosphates.

3.1.2. *Effect of the treatment with metal phosphate of the different biocatalyst on enzyme activity*

The biocatalysts were incubated with the three metal phosphates. Fig. 4S shows how the biocatalysts were colored depending on the salt, while all biocatalysts presented a similar color when submitted to the same mineralization protocol. Exceptions are the glutaraldehyde biocatalysts, where the initial brown colors make color identification difficult, except for copper.

Table 2 shows the effect of the treatment with the different metal phosphates in the enzyme activity versus the different substrates.

Using the octyl preparation, the activity decreased using *p*-NPB as substrate by 25 % using zinc, and by >40 % using copper or cobalt. The activity versus triacetin increased by around 50 % using zinc, while it almost remained unaltered using copper and cobalt. Using the methyl mandelates as substrates, the zinc salt promoted a 30 % decrease for both isomers, using copper the activity versus the *R*-isomer remains at 85 %, while versus the *S*-isomer it decreased below 60 %. Using cobalt,

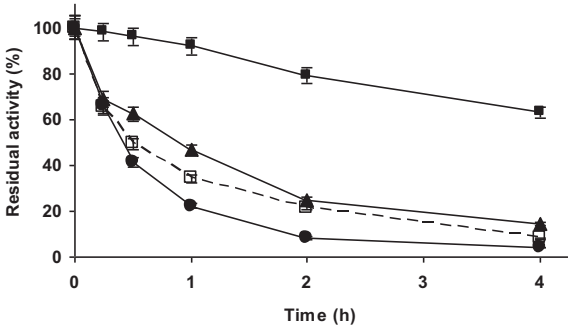

Fig. 4. Inactivation courses of differently mineralized TLL-octyl biocatalysts in 10 mM Tris-HCl buffer at pH 7.0 and 75 °C. Other specifications are described in Methods. Unmodified TLL-octyl (open squares and dotted line); TLL-octyl modified with $ZnCl_2$/sodium phosphate (solid squares); $CuCl_2$/sodium phosphate (solid circles); $CoCl_2$/sodium phosphate (solid triangles).

Table 2
Effect of the treatment with metallic salt/phosphate on the mass activity (immobilized biocatalyst) of the different biocatalyst. The hydrolytic activity was measured using 1 mM *p*-NPB, 50 mM triacetin, and 50 mM *R*- or *S*-methyl mandelate at pH 7.0 and 25 °C. Experiments were performed as described in methods.

Biocatalysts	Activity (U/g)														
	Without modification				Modification using $ZnCl_2$/sodium phosphate				Modification using $CuCl_2$/sodium phosphate				Modification using $CoCl_2$/sodium phosphate		
	p-NPB	Triacetin	*R*-Mandelate	*S*-Mandelate	*p*-NPB	Triacetin	*R*-Mandelate	*S*-Mandelate	*p*-NPB	Triacetin	*R*-Mandelate	*S*-Mandelate	*p*-NPB	Triacetin	*R*-Mandelate	*S*-Mandelate
TLL-octyl	1390.9 ± 25.0	110.9 ± 5.4	1.3 ± 0.06	0.7 ± 0.03	1069.43 ± 30.3	160.7 ± 7.2	0.9 ± 0.04	0.5 ± 0.02	797.6 ± 27.6	118.4 ± 4.8	1.1 ± 0.05	0.4 ± 0.02	784.0 ± 10.2	121.9 ± 5.1	0.8 ± 0.04	0.5 ± 0.02
Gly-TLL-VS-octyl	3279.0 ± 20.6	102.1 ± 4.1	1.2 ± 0.05	0.4 ± 0.02	3569.2 ± 125.2	119.3 ± 5.9	0.8 ± 0.03	0.2 ± 0.01	2411.7 ± 25.0	96.9 ± 3.6	0.8 ± 0.03	0.4 ± 0.02	3483.9 ± 12.1	119.7 ± 3.3	0.8 ± 0.03	0.3 ± 0.01
EDA-TLL-VS-octyl	3038.8 ± 51.7	83.6 ± 3.7	1.4 ± 0.02	0.3 ± 0.01	3505.6 ± 207.6	90.6 ± 3.1	0.7 ± 0.01	0.3 ± 0.01	3356.9 ± 86.8	130.6 ± 5.5	0.6 ± 0.03	0.3 ± 0.01	3902.8 ± 36.4	95.4 ± 4.8	0.8 ± 0.03	0.2 ± 0.01
TrisAEA-TLL-VS-octyl	3000.6 ± 28.3	94.0 ± 4.9	0.6 ± 0.02	0.07 ± 0.003	3540.2 ± 96.9	92.2 ± 4.7	0.7 ± 0.03	0.3 ± 0.01	2665.9 ± 159.1	64.8 ± 3.2	0.5 ± 0.02	0.4 ± 0.01	3611.2 ± 73.9	105.8 ± 4.1	0.5 ± 0.02	0.1 ± 0.004
Asp-TLL-VS-octyl	3109.6 ± 132.4	94.0 ± 3.7	0.5 ± 0.02	0.4 ± 0.02	3466.4 ± 141.8	143.4 ± 7.1	0.4 ± 0.01	0.4 ± 0.02	1934.9 ± 31.5	108.6 ± 5.4	0.2 ± 0.01	0.4 ± 0.02	3152.4 ± 170.4	126.0 ± 6.8	0.9 ± 0.04	0.4 ± 0.02
Cys-TLL-VS-octyl	2755.4 ± 98.1	64.1 ± 2.2	0.5 ± 0.02	0.2 ± 0.01	3470.4 ± 21.4	102.3 ± 5.4	0.4 ± 0.01	0.3 ± 0.02	2380.6 ± 85.6	90.9 ± 4.7	0.9 ± 0.04	0.4 ± 0.02	2006.0 ± 75.9	61.0 ± 3.0	0.8 ± 0.04	0.3 ± 0.01
TLL-Glu (pH 5.0)	37.6 ± 2.2	2.7 ± 0.1	10.6 ± 0.5	10.6 ± 0.5	32.4 ± 1.2	2.8 ± 0.1	5.4 ± 0.3	8.2 ± 0.4	57.4 ± 0.8	4.7 ± 0.2	2.4 ± 0.1	4.4 ± 0.2	21.1 ± 1.1	2.7 ± 0.1	3.4 ± 0.2	5.8 ± 0.3
TLL-Glu (pH 8.0)	15.6 ± 0.1	2.0 ± 0.1	9.1 ± 0.4	13.8 ± 0.7	24.0 ± 1.5	2.2 ± 0.1	8.9 ± 0.4	4.9 ± 0.2	25.0 ± 0.9	2.3 ± 0.1	0.9 ± 0.04	4.2 ± 0.2	18.0 ± 0.3	3.0 ± 0.1	1.0 ± 0.05	4.6 ± 0.2

the situation is the opposite, versus the *S*-isomer the activity decreased to 70 %, while the activity versus the *R*- decreased to 60 %.

Using the VS biocatalyst blocked with Gly, the treatment with zinc salts promoted the activity versus *p*-NPB to increase by <10 %, versus triacetin by almost 20 %, while the activity decreased versus both methyl mandelates. This effect of the zinc phosphate on enzyme activity and specificity is fully different to that found using octyl biocatalysts, where the activities decreased versus all substrates except triacetin. Using copper salts, the activity significantly decreased versus *p*-NPB (by 23 %) and *R*-methyl mandelate (by one third), remaining similar versus triacetin and *S*-methyl mandelate. The treatment with cobalt salts produced a slight increase on the activity versus *p*-NPB (by >6 %), increasing almost by 20 % versus triacetin, with a similar decrease in the enzyme activity versus both isomers of methyl mandelate. That way, the response to the modification with the different salts of Gly-TLL-VS-octyl-agarose is very different to those found using the octyl preparation. This could be due to the enzyme distortion caused by the covalent immobilization or the interactions of the enzyme with the support.

Next, we studied the effect of the metal modification of the EDA-TLL-VS-octyl biocatalysts activities. The treatment with zinc increased the activity versus *p*-NPB by 15 %, that way the zinc phospate- EDA-TLL-VS-octyl activity versus this substrate became similar to that of Zn phospate-Gly-TLL-VS-octyl. This treatment produced an increase of the activity versus triacetin (lower than 10 %) and *R*-methyl mandelate (50 %), while the activity versus *S*-methyl mandelate was maintained. When copper salts were used, the activity versus *p*-NPB increased by 10 % and versus triacetin by 50 % (becoming more active than TLL-octyl after any modification), and it remained unaltered for *S*-methyl mandelate while it decreased by >50 % for the *R*-isomer. Cobalt salts produced the highest increase in activity of this biocatalyst versus *p*-NPB (by almost 30 %, becoming the most active biocatalyst versus this substrate), the activity versus triacetin increased by 15 %, and the activities versus both methyl mandelate isomers decreased. Again, this was different to the effect of the mineralization using the octyl-agarose, but also using the Gly-TLL-VS-octyl. That means that the enzyme-support interactions played an important role on the modulation of the enzyme mineralization effects.

The effects of the modification of TrisEAE-TLL-VS-octyl biocatalyst offers a different picture. Zinc phosphate treatment again increased the activity versus *p*-NPB (by 18 %), maintaining the activities versus triacetin and *R*-methyl mandelate, while decreasing the activity by *S*-methyl mandelate (by almost 50 %). The copper treatment reduced the activity versus *p*-NPB (by >10 %), versus triacetin (by >30 %) and versus *R*- (by >15 %) and *S*- (by >40 %) methyl mandelate. Finally, the treatment with cobalt salt produced the highest increase in the activity versus *p*-NPB for this biocatalyst (over 20 %) and it also increased the activity versus triacetin (by 12 %), while it decreased the activity versus both methyl mandelate isomers, especially versus the *S*-isomer (maintaining only 14 % of the initial activity). In all cases, the treatment made that the biocatalyst recovered the preference by the *R*-isomer, in the case of the treatment with cobalt, the activities ratio become 5.

Using Asp as blocking reagent, the treatment with zinc salts permitted to increase the activity versus *p*-NPB (by >11 %), and very significantly with triacetin (by 50 %, becoming the most active biocatalyst versus this substrate). The activity versus the methyl mandelate isomers was almost maintained. Using copper phosphate, the activity versus *p*-NPB decreased by almost 40 %, versus triacetin it increased by >15 %, versus *S*-methyl mandelate it was maintained, but versus the *R*-isomer it decreased to 40 %. That way, this biocatalyst hydrolyzes the *S*-isomer twice as quickly as the *R*-isomer. The modification using the cobalt salt produced a small increase in the activity versus *p*-NPB, but the activity versus triacetin increased by almost 35 %. The activities versus *R*-methyl mandelate also increased, by 1.8 fold, while versus the *S*-isomer remained unaltered.

Also, the modification of Cys-TLL-VS-octyl with the different salts offers a new different situation. Using zinc salts, the activity increased by >25 % versus *p*-NPB, almost by 60 % using triacetin, and decreased the activity versus *R*-methyl mandelate (by 20 %) and increased the activity versus the *S*-isomer (by 40 %). Using copper salts, the activity decreased versus *p*-NPB (by <15 %), increased by >40 % versus triacetin, 1.8 fold versus *R*-methyl mandelate and 2 fold versus the *S*-isomer. Using cobalt salts, the activity decreased almost by 30 % versus *p*-NPB, 5 % versus triacetin, but increased by 60 % using *R*-methyl mandelate and 50 % using the *S*-isomer.

That way, the effect of the different mineralizations on the enzyme activity and specificities strongly depend on the blocking reagent. Considering that the enzyme orientation should be identical for all biocatalysts and also the number of enzyme-support linkages [96], this suggested that the enzyme-support interactions may be very relevant for the final effects of the mineralization, without discarding a role of the groups in the support in the metal phosphate crystal growth. Moreover, the metal phosphate treatment is able to tune the specificities of all the analyzed biocatalyst, each treatment favored some substrates while it is negative for others.

Next, we have analyzed the effect of the mineralization on the activity of both glutaraldehyde biocatalysts (Table 2). Here, the support surface is the same for both biocatalysts, but the enzyme orientation of the enzyme and the number of enzyme support bonds may be different (therefore, also the enzyme conformation) [82,85].

The modification with zinc salt of the biocatalyst immobilized at pH 5 produced a slight decrease on enzyme activity (by almost 15 %) while the biocatalyst prepared at pH 8 increased the activity by 50 %. Using triacetin as substrate, zinc mineralization did not present a relevant effect on enzyme activity, for the enzyme immobilized at pH 5 it increased by >3 %, while for the enzyme immobilized at pH 8 it increased by 10 %. Using the mandelate esters, the enzyme immobilized at pH 5 decreased the activity by almost 50 % for the *R*-isomer, and by 27 % for the *S*-isomer. The enzyme immobilized at pH 8 almost maintained the activity versus the *R*-isomer (from 9.1 U/g to 8.9 U/g), but it significantly decreased its activity versus the *S*-isomer (to just over 35 %). The modification with copper salt promoted a significant increase of the activity versus *p*-NPB of the enzyme immobilized at pH 5 (by >50 %) or at pH 8 (by 60 %), also the activity versus triacetin increased (by almost 75 % for the enzyme immobilized at pH 5 and by 15 % for the enzyme immobilized at pH 8). The activity versus *R*-methyl mandelate was strongly reduced, to 22 % using the enzyme immobilized at pH 5 and to 45 % for the enzyme immobilized at pH 8, and versus the *S*-isomer the results were also negative: the activity decreased to 40 % for the enzyme immobilized at pH 5 and to 30 % using the enzyme immobilized at pH 8. The modification with cobalt salts produced a decrease in the activity versus *p*-NPB of the enzyme immobilized at pH 5 (to 56 %) while it produced an increase for the enzyme immobilized at pH 8 (almost by 20 %). The activity versus triacetin of the enzyme immobilized at pH 5 remained unaltered, while the enzyme immobilized at pH 8 increased its activity versus this substrate by 50 % (becoming higher than the counterpart immobilized at pH 5). The activity versus *R*-methyl mandelate decreased due to this treatment, to 32 % for the enzyme immobilized at pH 5 and to 11 % for the enzyme immobilized at pH 8. Furthermore, the activity versus the *S*-isomer decreased by this mineralization, to <55 % for the enzyme immobilized at pH 5 and to around 33 % for the other biocatalyst.

Again, the effects of the mineralization strongly depended on the used biocatalysts. In this instance, the support surface is exactly the same, but the orientation and the number of enzyme linkages may be different. However, in all cases the mineralization permits to alter the enzyme specificity, increasing or decreasing the activity versus some substrates depending on the metal and the immobilization protocol.

Combining salts and immobilization protocol, it seems that the potential of TLL mineralization to tune the enzyme features may become really impressive.

3.1.3. Effect of the mineralization on enzyme stability

Fig. 4 shows the inactivation courses of the differently biocatalysts of TLL-octyl-agarose. As it has been previously reported [70], the stability of the enzyme strongly improved after modification with Zn^{2+}, while Cu^{2+} even promoted a slight destabilization and Co^{2+} treatment almost did not present any significant effect.

Using Gly-TLL-VS-octyl (Fig. 5a), Zn^{2+} treatment is also the most stabilizing treatment, however, the stabilization obtained using Co^{2+} is more significant than using the octyl biocatalyst, while Cu^{2+} maintained its destabilizing effect. Moving to EDA-TLL-VS-octyl (Fig. 5b), the results show that all salt treatments had no significant effects on enzyme stability. For TrisEAE-TLL-VS-octyl (Fig. 5c), all modifications presented a destabilizing effect, only relevant for Cu^{2+} that became a very destabilizing treatment for this enzyme formulation. Asp-TLL-VS-octyl (Fig. 5d) offered a new picture; now Co^{2+} and Zn^{2+} mineralization exhibited a strong stabilizing effect, very similar, while Cu^{2+} showed a small destabilizing effect. The situation is similar for Cys-TLL-VS-octyl (Fig. 5e), although in this case the destabilizing effect of Cu^{2+} mineralization is clearer. That way, as it occurred with the activity effects of the mineralization, the effects on enzyme stability of this enzyme modification strategy strongly depend on the blocking reagent (which alters the enzyme structure [96]).

The inactivation courses of the glutaraldehyde preparations are showed in Fig. 6. For the enzyme immobilized at pH 5 (Fig. 6a), Zn^{2+} and Co^{2+} treatment produced a strong stabilization, while Cu^{2+} produced a strong destabilization. If the enzyme is immobilized at pH 8 (Fig. 6b), Co^{2+} is the only mineralization that clearly improved the enzyme stability (in a lower extension that for the enzyme immobilized at pH 5), Zn^{2+} almost did not alter enzyme stability, while Cu^{2+} dramatically destabilized the enzyme. This confirmed that the enzyme orientation or number of enzyme-support bonds may be critical to determine the effect of the mineralization on the enzyme stability.

3.2. The case of CRL biocatalysts

3.2.1. Immobilization of CRL on the different supports

Fig. 5S shows the immobilization course of CRL on octyl-agarose. Around 80 % of the enzyme activity became immobilized in 2 h. The immobilization of the enzyme on octyl-VS maintained the immobilization yield in 80 % (Fig. 6S), and also the immobilization yield was very similar on glutaraldehyde at pH 5 and 8 (Fig. 7S).

Table 3 shows the activities of the different biocatalysts versus the 4 model substrates. CRL-octyl had the highest activity versus *p*-NPB, >11 fold higher than versus triacetin. That activity was <5 fold lower than

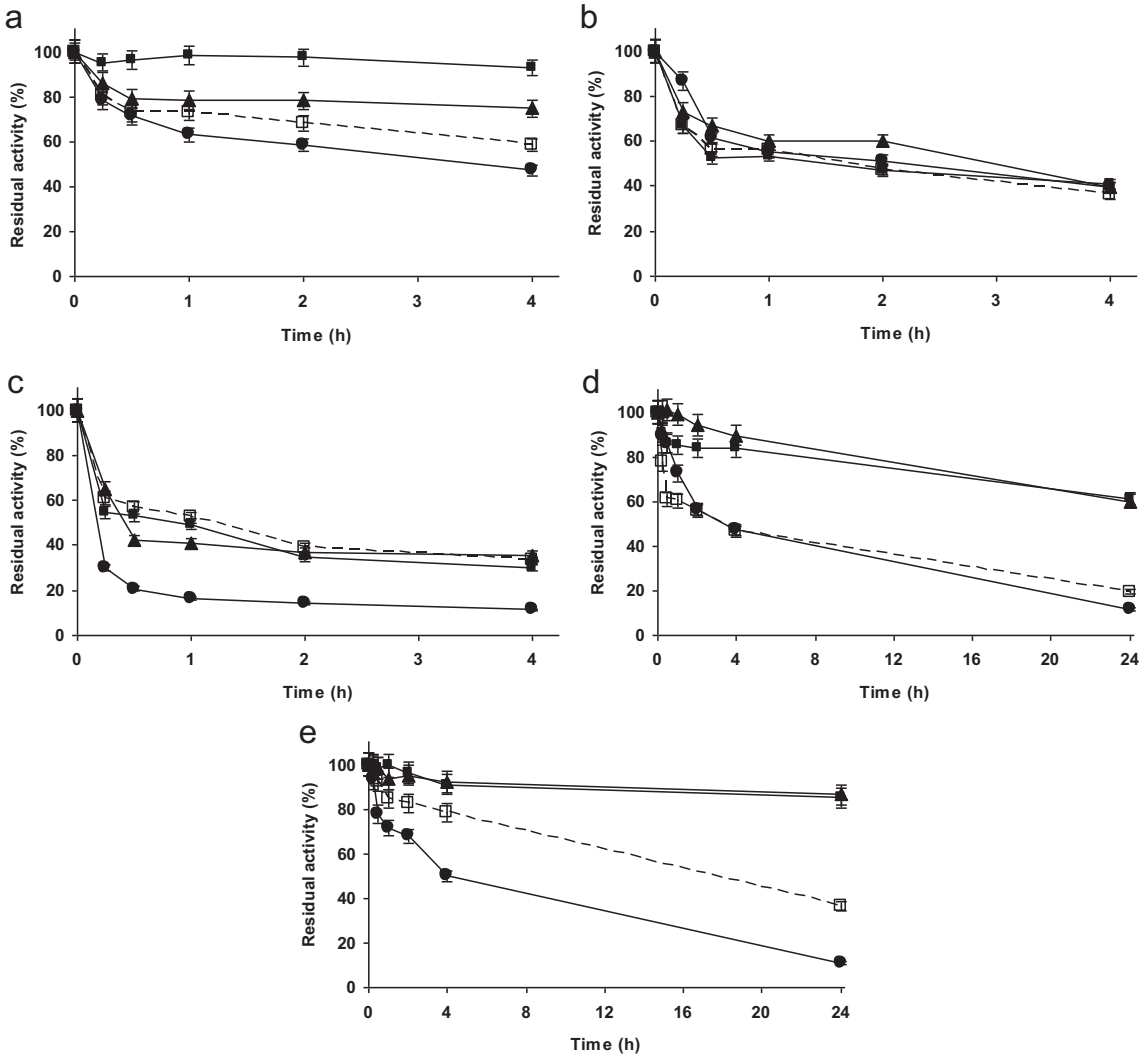

Fig. 5. Inactivation course of different TLL-VS-octyl biocatalysts modified with metallic salt/sodium phosphate: (a) Gly-TLL-VS-octyl, (b) EDA-TLL-VS-octyl, (c) TrisAEA-TLL-VS-octyl, (d) Asp-TLL-VS-octyl, (e) Cys-TLL-VS-octyl. The biocatalysts were inactivated at 75 °C, in presence of 10 mM Tris-HCl buffer at pH 7.0. Other specifications are described in Methods. Unmodified biocatalyst (open squares and dotted line); biocatalyst modified with $ZnCl_2$/sodium phosphate (solid squares); $CuCl_2$/sodium phosphate (solid circles); $CoCl_2$/sodium phosphate (solid triangles).

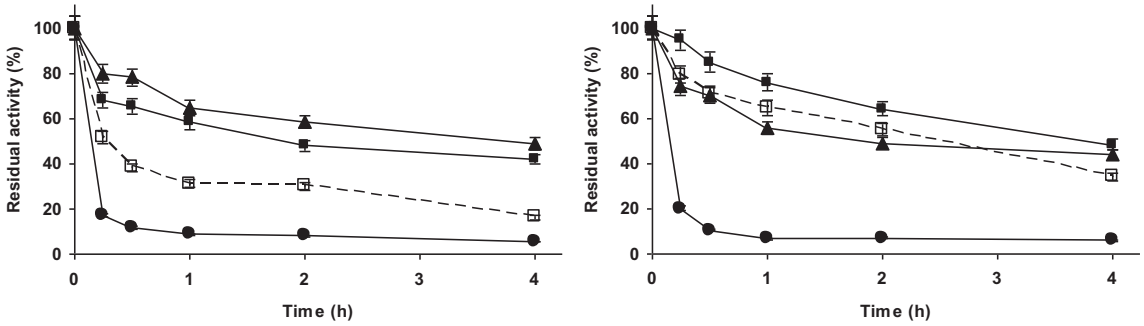

Fig. 6. Inactivation courses of differently mineralized TLL-Glu biocatalysts immobilized at (a) pH 5.0 and (b) pH 8.0. The biocatalysts were inactivated at 75 °C, in presence of 10 mM Tris-HCl buffer at pH 7.0. Other specifications are described in Methods. Unmodified TLL-Glu (open squares and dotted line); TLL-Glu modified with $ZnCl_2$/sodium phosphate (solid squares); $CuCl_2$/sodium phosphate (solid circles); $CoCl_2$/sodium phosphate (solid triangles).

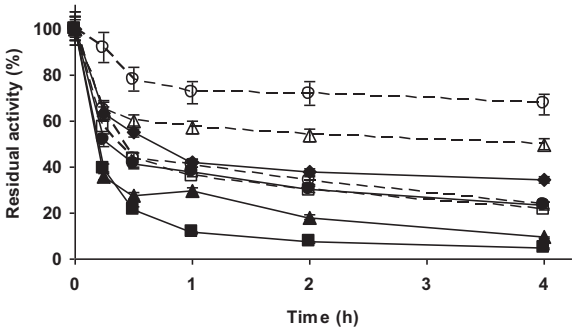

Fig. 7. Inactivation courses of different CRL biocatalysts in 10 mM Tris-HCl buffer at pH 7.0 and 70 °C. Other specifications are described in Methods. CRL-octyl (solid square and solid line); Gly-CRL-VS-octyl (solid rhombus and solid line); EDA-CRL-VS-ocyl (solid circles and solid line); TrisAEA-CRL-VS-octyl (solid triangles and solid line); Asp-CRL-VS-octyl (open squares and dotted line); Cys-CRL-VS-octyl (open rhombus and dotted line); CRL-Glu (pH 5.0) (open circles and dotted line); CRL-Glu (pH 8.0) (open triangles and dotted line).

Table 3
Mass activity (immobilized biocatalyst) of different CRL biocatalysts versus different substrates: 50 mM *R*- or *S*-methyl mandelate (pH 7 and 25 °C), 50 mM of triacetin (pH 7 and 25 °C) and 1 mM of *p*-NPB (pH 7 and 25 °C). Experiments were performed as described in methods.

Biocatalysts	Activity (U/g)			
	p-NPB	Triacetin	*R*-Mandelate	*S*-Mandelate
CRL-octyl	614.3 ± 36.7	49.3 ± 2.4	10.8 ± 0.5	3.9 ± 0.9
Gly-CRL-VS-octyl	1761.0 ± 58.6	0.7 ± 0.03	9.2 ± 0.5	3.4 ± 0.2
EDA-CRL-VS-octyl	1461.5 ± 28.3	0.5 ± 0.03	4.9 ± 0.2	3.4 ± 0.2
TrisAEA-CRL-VS-octyl	995.8 ± 14.5	0.3 ± 0.01	4.8 ± 0.2	4.0 ± 0.2
Asp-CRL-VS-octyl	1875.6 ± 91.68	0.7 ± 0.03	6.9 ± 0.3	4.1 ± 0.2
Cys-CRL-VS-octyl	1129.9 ± 49.7	0.3 ± 0.01	7.2 ± 0.2	4.4 ± 0.1
CRL-Glu (pH 5.0)	844.4 ± 25.69	36.8 ± 1.8	8.1 ± 0.5	8.8 ± 0.4
CRL-Glu (pH 8.0)	825.9 ± 10.8	27.1 ± 1.4	9.6 ± 0.5	11.1 ± 0.5

the activity versus *R*-methyl mandelate. The activities ratio with both isomers was almost 2.8.

The use of Gly-CRL-octyl biocatalyst permitted to greatly increase the activity versus *p*-NPB (by almost 2.9), while it promoted a drop in the activity versus triacetin (from >49 U/g to 0.7), slightly reducing the activities versus both isomers of methyl mandelate. Blocking the biocatalyst with EDA gave 2.4 higher *p*-NPB activity than the octyl biocatalyst, lowering the activity versus triacetin to 1 % and for *R*-methyl mandelate to 45 % and to 87 % for the *S*-isomer. The use of TrisAEA gave an increase on the *p*-NPB activity of 1.6 compared with the octyl preparation. The activity with triacetin was of only 0.3 U/g. Using *R*-methyl mandelate the activity decreased to <45 %, while with the *S*-isomer the activity marginally increased. Blocking the biocatalyst with Asp produced a biocatalyst 3 fold more active than the octyl biocatalyst using *p*-NPB, it reduced the activity versus *R*-methyl mandelate (to 64 %) while it slightly increased the activity versus the *S*-isomer (by a 5 %). Again the activity versus triacetin was strongly affected, maintaining only 0.7 U/g. The blocking with Cys gave an increase in activity versus *p*-NPB of 1.8 fold. The activity versus triacetin suffered a drop, maintaining only 0.3 U/g, while the activity versus *R*-methyl mandelate decreased by one third and the activity versus the *S*-isomer increased by >10 %. That way, the activities of the different biocatalyst prepared in octyl (VS) support were greatly different. Explanations for these results may be as described above for TLL. Again, we have built biocatalysts having different functional properties.

Focusing on the glutaraldehyde biocatalysts, the activity versus *p*-NPB was not very different for both biocatalysts, and it was 30–40 % higher than using CRL-octyl. The activity versus triacetin was higher for the biocatalyst immobilized at pH 5 than at pH 8 (35 % higher), but lower than the enzyme immobilized on octyl agarose (by >25 %). Both glutaraldehyde biocatalysts hydrolyzed the *S*- methyl mandelate more rapidly than the *R*-methyl mandelate. The enzyme immobilized at pH 5 was less active with both isomers (around 80 %) than the octyl preparation. However, the enzyme immobilized at pH 8 was less active versus the *R*-isomer than the octyl preparation (by >10 %), and more active versus the *S*-isomer (2.8 fold). That way, enzyme specificity and enantiospecificity were very different for the different biocatalysts. Again our objective has been accomplished.

Next, the enzyme stability of the different CRL biocatalysts was compared. Fig. 7 shows the inactivation courses of the different CRL-biocatalysts. CRL-octyl is the least stable biocatalyst, being the enzyme immobilized on glutaraldehyde at pH 8 less stable than the enzyme immobilized at pH 5, even though at pH 8 a higher number of enzyme-supports bonds may be expected. This suggests that the immobilization pH may alter the enzyme orientation on the support, as enzyme orientation also alters the effects of the immobilization on enzyme stability [84–87,89,90,92–94,113], and the immobilization achieved at pH 5 seems to involve more relevant areas for the enzyme stability [114,115]. The VS-octyl biocatalysts stabilities are in between the glutaraldehyde and the octyl biocatalyst, without too large differences (the blocking with TrisAEA produced the least stable biocatalysts, while the blocking with Gly gave the most stable preparation).

That way, again the functional properties of the different biocatalysts

were quite different, and these biocatalysts were used for mineralization using diverse salts.

3.2.2. Effect of the treatment with metal phosphate of the different biocatalyst on enzyme activity

The different biocatalysts were treated with the different salts, Fig. 8S shows that the colors were similar to those observed using TLL. Table 4 offers the effect of the mineralization of the biocatalyst on their activities versus the different substrates.

Starting with CRL-octyl, the use of zinc salts produced an increase of its *p*-NPB activity by around 10 %, it decreased the activity versus triacetin by 30 % and versus both methyl mandelate isomers by around 10 %. Using copper salts, the increase on the activity with *p*-NPB is almost 15 %, activities versus triacetin and *R*-methyl mandelate are fairly maintained and the activity versus *S*-methyl mandelate decreased by almost 20 %. Cobalt phosphate mineralization increased the activity versus *p*-NPB (by <5 %), and decreased the activity versus triacetin (to 83 %), *R*- (to 88 %) and *S*- (to 75 %) methyl mandelate.

The situation is different using Gly-CRL-VS-octyl, the modification with zinc phosphate had marginal effects on the enzyme activity, slightly decreased the activity versus *p*-NPB and *S*-methyl mandelate (to 95 %), it maintained the activity versus triacetin, and increased the activity versus *R*-methyl mandelate (by 5 %). The use of copper salts also produced marginal effects on the biocatalysts features, while cobalt mineralization increased the activity versus *p*-NPB (by 12 %), *R*- and *S*-methyl mandelate (by >7 %), while the activity versus triacetin remained unaltered. Similar small increases or decreases in activities could be detected for the other CRL-VS-octyl biocatalysts, never exceeding 15 %. It seemed that the mineralization presented a much smaller effect for these CRL biocatalysts than when using TLL.

The changes on enzyme activity induced by the mineralization using the glutaraldehyde biocatalysts were clearer. The enzyme immobilized at pH 5 slightly decreased its *p*-NPB activity after zinc mineralization, while the enzyme immobilized at pH 8 slightly increased its activity. Using triacetin, the enzyme immobilized at pH 5 increased its activity by 33 %; if the enzyme was immobilized at pH 8, the increase on the activity is by 65 %. If *R*-methyl mandelate was used as substrate, the activity of the enzyme immobilized at pH 5 marginally increased, while the enzyme immobilized at pH 8 decreased its activity by >5 %. Using the *S*-isomer, the enzyme immobilized at pH 5 increased the activity after this mineralization by 8 %, while if the immobilization was performed at pH 8, the activity decreased to <80 %.

Analyzing the effects of the copper salts treatment, the activity versus *p*-NPB decreased almost by 10 % for the enzyme immobilized at pH 5, while the enzyme immobilized at pH 8 lost one third of the activity. Using triacetin as substrate, the enzyme immobilized at pH 5 decreased the activity to <50 %, the other biocatalyst only lost 10 % of the activity.

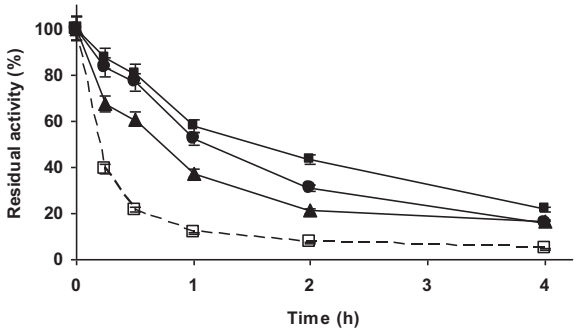

Fig. 8. Inactivation courses of differently mineralized CRL-octyl biocatalysts in 10 mM Tris-HCl buffer at pH 7.0 and 70 °C. Other specifications are described in Methods. Unmodified CRL-octyl (open squares and dotted line); CRL-octyl modified with $ZnCl_2$/sodium phosphate (solid squares); $CuCl_2$/sodium phosphate (solid circles); $CoCl_2$/sodium phosphate (solid triangles).

Table 4
Effect of the treatment with metallic salt/phosphate on the activity of the different CRL biocatalyst versus different substrates. The hydrolytic activity was measured using 1 mM *p*-NPB, 50 mM triacetin, and 50 mM *R*- or *S*-methyl mandelate at pH 7.0 and 25 °C. Experiments were performed as described in methods.

Biocatalysts	Activity (U/g)														
	Without modification				Modification using $ZnCl_2$/sodium phosphate				Modification using $CuCl_2$/sodium phosphate				Modification using $CoCl_2$/sodium phosphate		
	p-NPB	Triacetin	*R*-Mandelate	*S*-Mandelate	*p*-NPB	Triacetin	*R*-Mandelate	*S*-Mandelate	*p*-NPB	Triacetin	*R*-Mandelate	*S*-Mandelate	*p*-NPB	Triacetin	*R*-Mandelate	*S*-Mandelate
CRL-octyl	614.3 ± 36.7	49.3 ± 2.4	10.8 ± 0.5	3.9 ± 0.9	675.7 ± 29.4	34.5 ± 1.7	9.6 ± 0.5	3.5 ± 0.1	701.6 ± 25.1	51.1 ± 2.6	9.9 ± 0.5	3.2 ± 0.2	639.4 ± 23.2	40.89 ± 2.1	9.5 ± 0.5	2.9 ± 0.1
Gly-CRL-VS-octyl	1761.0 ± 58.6	0.7 ± 0.03	9.2 ± 0.5	3.4 ± 0.2	1674.7 ± 48.2	0.7 ± 0.03	9.7 ± 0.5	3.6 ± 0.2	1628.4 ± 8.08	0.5 ± 0.02	9.1 ± 0.4	3.3 ± 0.1	1974.1 ± 10.5	0.7 ± 0.02	9.9 ± 0.5	3.6 ± 0.2
EDA-CRL-VS-octyl	1461.5 ± 28.3	0.5 ± 0.03	4.9 ± 0.2	3.4 ± 0.2	1461.1 ± 12.92	0.5 ± 0.03	4.7 ± 0.4	3.5 ± 0.2	1276.73 ± 21.8	0.5 ± 0.02	4.5 ± 0.3	3.6 ± 0.2	1630.8 ± 9.69	0.5 ± 0.02	5.1 ± 0.4	3.9 ± 0.2
TrisAEA-CRL-VS-octyl	995.8 ± 14.5	0.3 ± 0.01	4.8 ± 0.2	4.0 ± 0.2	1067.5 ± 40.9	0.4 ± 0.01	4.6 ± 0.3	4.0 ± 0.3	1012.5 ± 29.48	0.4 ± 0.02	4.8 ± 0.2	4.0 ± 0.2	941.86 ± 30.9	0.3 ± 0.01	5.0 ± 0.3	4.1 ± 0.2
Asp-CRL-VS-octyl	1875.6 ± 91.68	0.7 ± 0.03	6.9 ± 0.3	4.1 ± 0.2	1721.7 ± 46.1	0.8 ± 0.03	7.5 ± 0.4	4.0 ± 0.2	1860.2 ± 56.5	0.8 ± 0.03	7.0 ± 0.4	3.9 ± 0.2	1813.9 ± 70.3	0.8 ± 0.03	7.0 ± 0.4	4.1 ± 0.2
Cys-CRL-VS-octyl	1129.9 ± 49.7	0.3 ± 0.01	7.2 ± 0.2	4.4 ± 0.1	1153.1 ± 43.2	0.4 ± 0.01	6.9 ± 0.3	4.8 ± 0.2	994.32 ± 63.8	0.3 ± 0.01	7.5 ± 0.4	4.3 ± 0.1	1122.2 ± 70.9	0.4 ± 0.02	7.4 ± 0.3	4.5 ± 0.3
CRL-Glu (pH 5.0)	844.4 ± 25.69	36.8 ± 1.8	8.1 ± 0.5	8.8 ± 0.4	835.7 ± 35.7	48.5 ± 2.4	8.3 ± 0.3	9.5 ± 0.5	777.4 ± 23.8	17.2 ± 0.9	7.8 ± 0.3	7.6 ± 0.4	853.2 ± 20.2	46.9 ± 2.3	8.5 ± 0.5	9.4 ± 0.5
CRL-Glu (pH 8.0)	825.9 ± 10.8	27.1 ± 1.4	9.6 ± 0.5	11.1 ± 0.5	849.1 ± 31.5	44.9 ± 2.3	8.1 ± 0.4	8.8 ± 0.4	550.5 ± 23.2	18.8 ± 0.9	8.0 ± 0.4	7.8 ± 0.4	701.6 ± 16.3	44.9 ± 2.2	7.8 ± 0.4	7.9 ± 0.4

Both biocatalysts decreased their activities versus both methyl mandelate, but more for the *S*- than for the *R*-isomer. The activities ratios became inverted after the treatment, now the immobilized and copper mineralized enzyme preferred the *R*-isomer.

Finally, using cobalt salts, the activity versus *p*-NPB marginally increased for the enzyme immobilized at pH 5, the increase is more significant for its triacetin activity (by 27 %). For *R*- and *S*-methyl mandelate, the increase in activity is small (5 and 7 %). The enzyme immobilized at pH 8 decreased its *p*-NPB activity to 85 %, while it increased its triacetin activity by 1.65 fold. Using methyl mandelate, the activity decreased for both isomers, more for the *S*-isomer.

That way, although not as significant as in the case of TLL, the combination of immobilization protocol and mineralization salt permitted to tune the specificity and activity of immobilized CRL.

3.2.3. *Effect of the mineralization on enzyme stability*

Next, the effect of the mineralization on the biocatalysts stability was analyzed. Using CRL-octyl (Fig. 8), all mineralized biocatalysts were more stable than the unmodified octyl, being the biocatalyst modified with cobalt salts less stabilized than using the other salts and that biocatalyst modified with zinc salts was the most stable. The situation was fairly different using Gly-CRL-VS-octyl (Fig. 9a), where the copper salt produced an enzyme destabilization and the stabilization obtained using zinc phosphate is much smaller than using the octyl biocatalyst. For EDA-CRL-VS-octyl (Fig. 9b), the treatments had a moderate effect on enzyme stability, slightly negative, being more destabilizing the mineralization using copper. TrisAEA-CRL-VS-octyl (Fig. 9c) stability was not affected by the treatments, except using copper, which had a negative effect. Asp-CRL-VS-octyl (Fig. 9d) and Cys- CRL-VS-octyl (Fig. 9e) was slightly stabilized using cobalt and zinc salts, and marginally destabilized using copper salts.

Moving to the glutaraldehyde biocatalyst, the differences caused by the immobilization pH are very clear. While the stability of the enzyme immobilized at pH 5 (Fig. 10a) was almost not affected by the mineralization using cobalt and zinc salts, copper produced a drastic destabilization. Using the enzyme immobilized at pH 8 (Fig. 10b), the zinc salt produced a clear stabilization, followed by the cobalt salt, while the copper mineralization produced an enzyme destabilization, although less relevant than using the enzyme immobilized at pH 5.

That way, the mineralization effect on enzyme stability on immobilized CRL strongly depended on the immobilization protocol. In some instances, a mineralization protocol produced a great stabilization, while in others the same protocol even produced a negative effect. Using CRL, the effects may be less significant than using TLL, but they are still

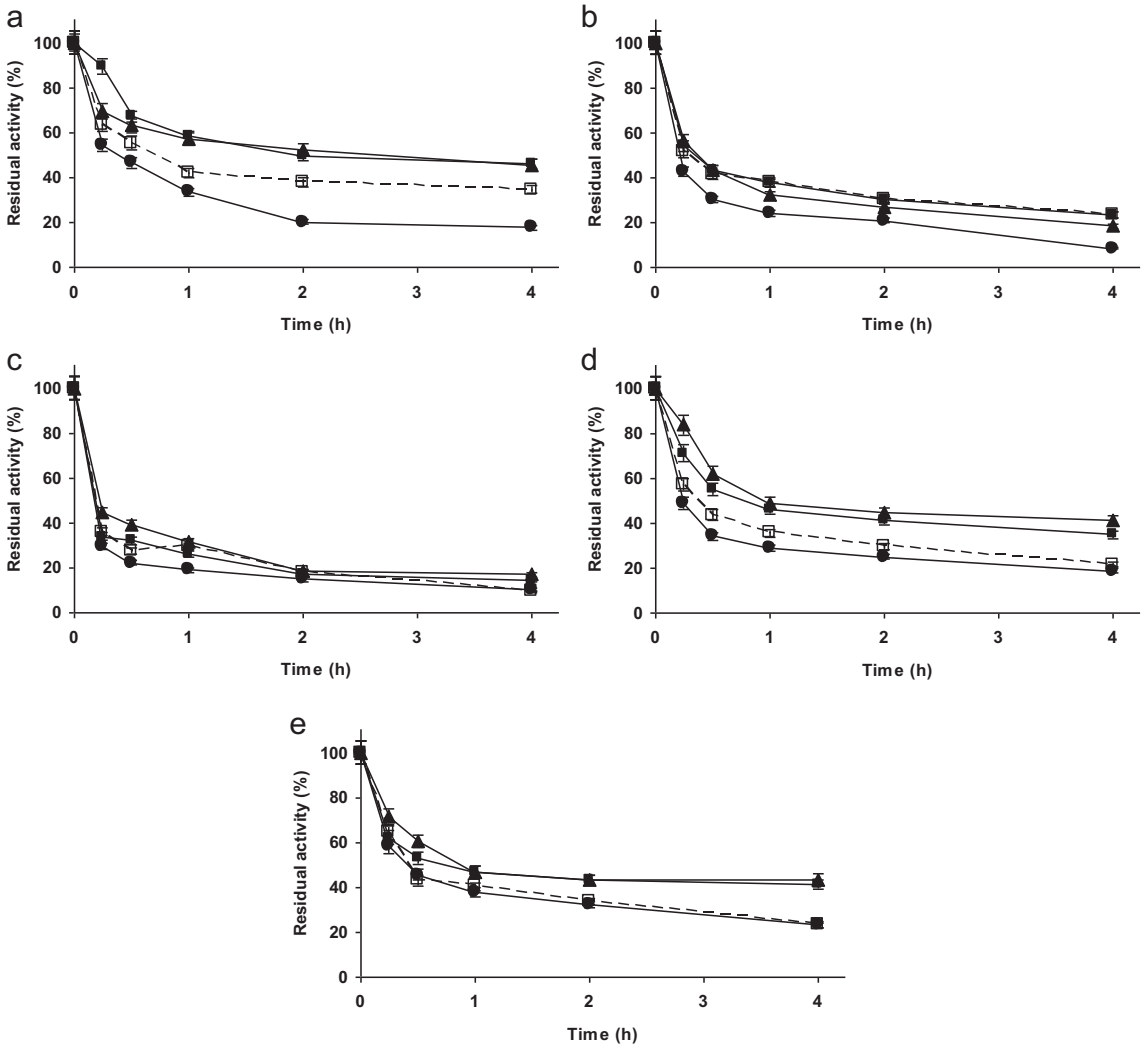

Fig. 9. Inactivation course of different CRL-VS-octyl biocatalysts modified with different metallic salt/sodium phosphate: (a) Gly-CRL-VS-octyl, (b) EDA-CRL-VS-octyl, (c) TrisAEA-CRL-VS-octyl, (d) Asp-CRL-VS-octyl, (e) Cys-CRL-VS-octyl. The biocatalysts were inactivated at 70 °C, in presence of 10 mM Tris-HCl buffer at pH 7.0. Other specifications are described in Methods. Unmodified biocatalyst (open squares and dotted line); biocatalyst modified with $ZnCl_2$/sodium phosphate (solid squares); $CuCl_2$/sodium phosphate (solid circles); $CoCl_2$/sodium phosphate (solid triangles).

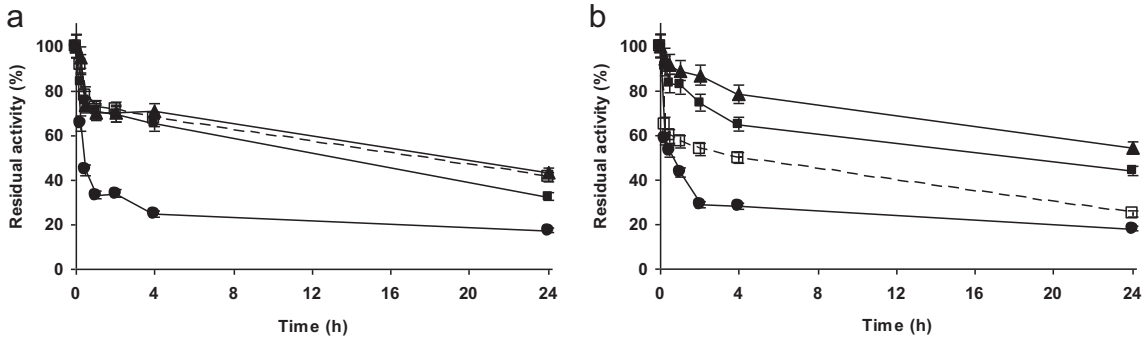

Fig. 10. Inactivation courses of CRL-Glu biocatalysts immobilized at (a) pH 5.0 and (b) pH 8.0. The biocatalysts were inactivated at 70 °C, in presence of 10 mM Tris-HCl buffer at pH 7.0. Other specifications are described in Methods. Unmodified CRL-Glu (open squares and dotted line); CRL-Glu modified with $ZnCl_2$/sodium phosphate (solid squares); $CuCl_2$/sodium phosphate (solid circles); $CoCl_2$/sodium phosphate (solid triangles).

very relevant.

3.3. Operational stability of the biocatalysts in hydrolysis of methyl mandelic esters

Although the objective of this paper was not to optimize any reaction, all the biocatalysts were reused 3 times in hydrolysis cycles of methyl mandelate hydrolysis (both *R*- and *S*-isomers). The activities of all biocatalysts were maintained during the 3 cycles over 95 % (nor shown results), as expected from the high stability of the octyl-lipase and glutaraldehyde-lipase preparations, even the destabilized biocatalysts maintained their activities under these mild conditions. Moreover, the color induced by the metal was maintained also almost intact after these 3 reuses.

4. Conclusion

The results shown in this paper are new examples on the power of enzyme immobilization to tune enzyme functional features, including examples where the only difference is the final physical interactions between enzyme and support (i.e., octyl-vinyl sulfone biocatalysts blocked with different reagents). Now, we have clearly shown how the immobilization protocol determines the effect on enzyme functional properties of enzyme mineralization using metal phosphates. This occurs even if the only difference between the different biocatalysts is the groups located surface of the support, and therefore, the enzyme-support interactions. Changes on enzyme stability or activity versus a specific substrate caused by the mineralization using a specific metal salt may be positive or negative depending on the immobilization protocol. In the used examples, TLL seems to be more responsible to these changes than CRL, but in both cases the differences are significant enough. This means that to select the best immobilization protocol/enzyme/mineralization protocol, the researcher should analyze the final enzyme features in the specific process where the enzyme will be utilized (substrate, reaction conditions).

This simple strategy opens the door to integrate enzyme immobilization and enzyme mineralization to increase the library of biocatalysts from a single lipase that can be available to optimize each specific process. Moreover, this suggests that the results obtained by mineralization of a specific immobilized biocatalyst cannot be directly extrapolated to other biocatalysts.

The use a wide battery of metals and immobilization protocols can permit to "create biocatalysts" adequate for many processes, even if the original enzyme does not look very adequate for the specific process [47,116].

It could be highly interesting to investigate the different structural changes that the enzyme can adopt as consequence of its interaction with the different support surfaces, as this can give some clues of the reasons for the different activities and stabilities of the biocatalysts [96].

The potential of biophysical, physic-chemical and spectroscopic techniques to advance in the structural analysis of immobilized enzymes and understand the structure-function relationship of the enzymes is advancing very rapidly and their potential (today still they have some limitations) [117,118], to improve the understanding the phenomena that determine the final properties of the immobilized enzyme may open new opportunities in the development more controllable and efficient immobilization process [117–126]. Although the future of these techniques gives us a reason to be optimistic, the current scenario is they are still far from can purpose a clear finger-printing that can explain the functional features of an immobilized enzymes.

Author statement

José R. Guimarães, Diego Carballares performed the experiments. Javier Rocha-Martin co-designed and co-supervised the immobilization of the immobilized enzymes. Roberto Fernandez-Lafuente and Paulo W. Tardioli co-designed and co-supervised the experiments. All authors contributed to the writing and final editing of the paper.

Declaration of competing interest

The authors declare that they have no known competing financial interests or personal relationships that could have appeared to influence the work reported in this paper.

Acknowledgments

We gratefully recognize the financial support from Coordenação de Aperfeiçoamento de Pessoal de Nível Superior–Brasil (CAPES, Finance Code 001; CAPES-PRINT, number 88887.571985/2020-00), MCIN/AEI/10.13039/501100011033 (PID2021-122398OB-I00). DC thanks to Ministerio de Ciencia e Innovación-Spanish Government by a FPI. The help and suggestions from Dr. Ángel Berenguer (Departamento de Química Inorgánica, Universidad de Alicante) are gratefully recognized.

Appendix A. Supplementary data

Supplementary data to this article can be found online at https://doi.org/10.1016/j.ijbiomac.2022.10.030.

References

[1] K.-E. Jaeger, T. Eggert, Lipases for biotechnology, Curr. Opin. Biotechnol. 13 (2002) 390–397, https://doi.org/10.1016/S0958-1669(02)00341-5.
[2] K. Jaeger, Microbial lipases form versatile tools for biotechnology, Trends Biotechnol. 16 (1998) 396–403, https://doi.org/10.1016/S0167-7799(98)01195-0.

[3] P. Reis, K. Holmberg, H. Watzke, M.E. Leser, R. Miller, Lipases at interfaces: a review, Adv. Colloid Interf. Sci. 147–148 (2009) 237–250, https://doi.org/10.1016/j.cis.2008.06.001.
[4] M.T. Reetz, Lipases as practical biocatalysts, Curr. Opin. Chem. Biol. 6 (2002) 145–150, https://doi.org/10.1016/S1367-5931(02)00297-1.
[5] P. Villeneuve, J.M. Muderhwa, J. Graille, M.J. Haas, Customizing lipases for biocatalysis: a survey of chemical, physical and molecular biological approaches, J. Mol. Catal. B Enzym. 9 (2000) 113–148, https://doi.org/10.1016/S1381-1177(99)00107-1.
[6] X. Xu, Production of specific-structured triacylglycerols by lipase-catalyzed reactions: a review, Eur. J. Lipid Sci. Technol. 102 (2000) 287–303, https://doi.org/10.1002/(SICI)1438-9312(200004)102:4<287::AID-EJLT287>3.0.CO;2-Q.
[7] A. Ghanem, Trends in lipase-catalyzed asymmetric access to enantiomerically pure/enriched compounds, Tetrahedron 63 (2007) 1721–1754, https://doi.org/10.1016/j.tet.2006.09.110.
[8] P. Stergiou, A. Foukis, M. Filippou, M. Koukouritaki, M. Parapouli, L. G. Theodorou, E. Hatziloukas, A. Afendra, A. Pandey, E.M. Papamichael, Advances in lipase-catalyzed esterification reactions, Biotechnol. Adv. 31 (2013) 1846–1859, https://doi.org/10.1016/j.biotechadv.2013.08.006.
[9] R.R. Sousa, A.S.A. Silva, R. Fernandez-Lafuente, V.S. Ferreira-Leitão, Solvent-free esterifications mediated by immobilized lipases: a review from thermodynamic and kinetic perspectives, Catal. Sci. Technol. 11 (2021) 5696–5711, https://doi.org/10.1039/d1cy00696g.
[10] M. Kapoor, M.N. Gupta, Lipase promiscuity and its biochemical applications, Process Biochem. 47 (2012) 555–569, https://doi.org/10.1016/j.procbio.2012.01.011.
[11] B.P. Dwivedee, S. Soni, M. Sharma, J. Bhaumik, J.K. Laha, U.C. Banerjee, Promiscuity of lipase-catalyzed reactions for organic synthesis: a recent update, Chem. Sel. 3 (2018) 2441–2466, https://doi.org/10.1002/slct.201702954.
[12] A. Patti, C. Sanfilippo, Stereoselective promiscuous reactions catalyzed by lipases, Int. J. Mol. Sci. 23 (2022) 2675, https://doi.org/10.3390/ijms23052675.
[13] V.D. Nimkande, A. Bafana, A review on the utility of microbial lipases in wastewater treatment, J. Water Process Eng. 46 (2022), 102591, https://doi.org/10.1016/j.jwpe.2022.102591.
[14] D. Remonatto, R.H. Miotti Jr., R. Monti, J.C. Bassan, A.V. de Paula, Applications of immobilized lipases in enzymatic reactors: a review, Process Biochem. 114 (2022) 1–20, https://doi.org/10.1016/j.procbio.2022.01.004.
[15] R.N. Vilas Bôas, H.F. Castro, A review of synthesis of esters with aromatic, emulsifying, and lubricant properties by biotransformation using lipases, Biotechnol. Bioeng. 119 (2022) 725–742, https://doi.org/10.1002/bit.28024.
[16] C.A. Salgado, C.I.A. dos Santos, M.C.D. Vanetti, Microbial lipases: propitious biocatalysts for the food industry, Food Biosci. 45 (2022), 101509, https://doi.org/10.1016/j.fbio.2021.101509.
[17] A.da S. Pereira, A.H. de Souza, J.L. Fraga, P. Villeneuve, A.G. Torres, P.F. F. Amaral, Lipases as effective green biocatalysts for phytosterol esters' production: a review, Catalysts 12 (2022) 88, https://doi.org/10.3390/catal12010088.
[18] I.C.A. Bolina, R.A.B. Gomes, A.A. Mendes, Biolubricant production from several oleaginous feedstocks using lipases as catalysts: current scenario and future perspectives, BioEnergy Res. (2021), https://doi.org/10.1007/s12155-020-10242-4.
[19] S. Verma, R.N. Choudhary, A.P. Kanadje, U.C. Banerjee, Diversifying arena of drug synthesis: in the realm of lipase mediated waves of biocatalysis, Catalysts 11 (2021) 1328, https://doi.org/10.3390/catal11111328.
[20] H.E. Schoemaker, D. Mink, M.G. Wubbolts, Dispelling the myths-biocatalysis in industrial synthesis, Science 299 (2003) 1694–1697, https://doi.org/10.1126/science.1079237.
[21] M. Ferrer, R. Bargiela, M. Martínez-Martínez, J. Mir, R. Koch, O.V. Golyshina, P. N. Golyshin, Biodiversity for biocatalysis: a review of the α/β-hydrolase fold superfamily of esterases-lipases discovered in metagenomes, Biocatal. Biotransformation 33 (2015) 235–249, https://doi.org/10.3109/10242422.2016.1151416.
[22] C. Peña-García, M. Martínez-Martínez, D. Reyes-Duarte, M. Ferrer, High throughput screening of esterases, lipases and phospholipases in mutant and metagenomic libraries: a review, Comb. Chem. High Throughput Screen. 19 (2016) 605–615, https://doi.org/10.2174/1386207319666151110123927.
[23] J.M. Almeida, R.C. Alnoch, E.M. Souza, D.A. Mitchell, N. Krieger, Metagenomics: is it a powerful tool to obtain lipases for application in biocatalysis? 1868 (2020), 140320, https://doi.org/10.1016/j.bbapap.2019.140320.
[24] S. Verma, G.K. Meghwanshi, R. Kumar, Current perspectives for microbial lipases from extremophiles and metagenomics, Biochimie 182 (2021) 23–36, https://doi.org/10.1016/j.biochi.2020.12.027.
[25] Z. Jiang, C. Zhang, M. Tang, B. Xu, L. Wang, W. Qian, J. He, Z. Zhao, Q. Wu, Y. Mu, J. Ding, R. Zhang, Z. Huang, N. Han, Improving the thermostability of rhizopus chinensis lipase through site-directed mutagenesis based on B-factor analysis, Front. Microbiol. 11 (2020) 1–8, https://doi.org/10.3389/fmicb.2020.00346.
[26] R.A. Mohamed, A.B. Salleh, T.C. Leow, N.M. Yahaya, M.B. Abdul Rahman, Site-directed mutagenesis: role of lid region for T1 lipase specificity, Protein Eng. Des. Sel. 31 (2018) 221–229, https://doi.org/10.1093/protein/gzy023.
[27] M. Mohammadi, Z. Sepehrizadeh, A. Ebrahim-Habibi, A.R. Shahverdi, M. A. Faramarzi, N. Setayesh, Enhancing activity and thermostability of lipase a from Serratia marcescens by site-directed mutagenesis, Enzym. Microb. Technol. 93–94 (2016) 18–28, https://doi.org/10.1016/j.enzmictec.2016.07.006.
[28] H. Chen, J.-P. Wu, L.-R. Yang, G. Xu, Improving Pseudomonas alcaligenes lipase's diastereopreference in hydrolysis of diastereomeric mixture of menthyl propionate by site-directed mutagenesis, Biotechnol. Bioprocess Eng. 19 (2014) 592–604, https://doi.org/10.1007/s12257-014-0066-9.
[29] R.D. Joerger, M.J. Haas, Alteration of chain length selectivity of a rhizopus delemar lipase through site-directed mutagenesis, Lipids 29 (1994) 377–384, https://doi.org/10.1007/BF02537305.
[30] D. Li, X. Chen, Z. Chen, X. Lin, J. Xu, Q. Wu, Directed evolution of lipase a from Bacillus subtilis for the preparation of enantiocomplementary sec-alcohols, Green Synth. Catal. 2 (2021) 290–294, https://doi.org/10.1016/j.gresc.2021.07.003.
[31] M. Zhang, Q. Li, X. Lan, X. Li, Y. Zhang, Z. Wang, J. Zheng, Directed evolution of aspergillus oryzae lipase for the efficient resolution of (R, S)-ethyl-2-(4-hydroxyphenoxy) propanoate, Bioprocess Biosyst. Eng. 43 (2020) 2131–2141, https://doi.org/10.1007/s00449-020-02393-7.
[32] L. Guan, Y. Gao, J. Li, K. Wang, Z. Zhang, S. Yan, N. Ji, Y. Zhou, S. Lu, Directed evolution of Pseudomonas fluorescens lipase variants with improved thermostability using error-prone PCR, Front. Bioeng. Biotechnol. 8 (2020), 602138, https://doi.org/10.3389/fbioe.2020.01034.
[33] J. Wang, R. Bai, N. Wu, Y. Zhang, L. Hu, Effect of propeptide mutations on the directed evolution of rhizomucor miehei lipase, Protein Pept. Lett. 29 (2022) 360–369, https://doi.org/10.2174/0929866529666220314105130.
[34] C. Mateo, J.M. Palomo, G. Fernandez-Lorente, J.M. Guisan, R. Fernandez-Lafuente, Improvement of enzyme activity, stability and selectivity via immobilization techniques, Enzym. Microb. Technol. 40 (2007) 1451–1463, https://doi.org/10.1016/j.enzmictec.2007.01.018.
[35] C. Garcia-Galan, Á. Berenguer-Murcia, R. Fernandez-Lafuente, R.C. Rodrigues, Potential of different enzyme immobilization strategies to improve enzyme performance, Adv. Synth. Catal. 353 (2011) 2885–2904, https://doi.org/10.1002/adsc.201100534.
[36] A. Lorente-Arevalo, M. Ladero, J.M. Bolivar, Intensification of oxygen-dependent biotransformations catalyzed by immobilized enzymes, Curr. Opin. Green Sustain. Chem. 32 (2021), 100544, https://doi.org/10.1016/j.cogsc.2021.100544.
[37] J. Bié, B. Sepodes, P.C.B. Fernandes, M.H.L. Ribeiro, Enzyme immobilization and co-immobilization: main framework, advances and some applications, Processes 10 (2022) 494, https://doi.org/10.3390/pr10030494.
[38] D.N. Tran, K.J. Balkus, Perspective of recent progress in immobilization of enzymes, ACS Catal. 71 (2011) 956–968, https://doi.org/10.1163/1568525X-12342362.
[39] R.K. Singh, M.K. Tiwari, R. Singh, J.-K. Lee, From protein engineering to immobilization: promising strategies for the upgrade of industrial enzymes, Int. J. Mol. Sci. 14 (2013) 1232–1277, https://doi.org/10.3390/ijms14011232.
[40] Y. Zhang, J. Ge, Z. Liu, Enhanced activity of immobilized or chemically modified enzymes, ACS Catal. 5 (2015) 4503–4513, https://doi.org/10.1021/acscatal.5b00996.
[41] R.A. Sheldon, A. Basso, D. Brady, New frontiers in enzyme immobilisation: robust biocatalysts for a circular bio-based economy, Chem. Soc. Rev. 50 (2021) 5850–5862, https://doi.org/10.1039/D1CS00015B.
[42] R.C. Rodrigues, Á. Berenguer-Murcia, D. Carballares, R. Morellon-Sterling, R. Fernandez-Lafuente, Stabilization of enzymes via immobilization: multipoint covalent attachment and other stabilization strategies, Biotechnol. Adv. 52 (2021), 107821, https://doi.org/10.1016/j.biotechadv.2021.107821.
[43] J.M. Bolivar, F. López-Gallego, Characterization and evaluation of immobilized enzymes for applications in flow reactors, Curr. Opin. Green Sustain. Chem. 25 (2020), 100349, https://doi.org/10.1016/j.cogsc.2020.04.010.
[44] H.-J. Federsel, T.S. Moody, S.J.C. Taylor, Recent trends in enzyme immobilization—concepts for expanding the biocatalysis toolbox, Molecules 26 (2021) 2822, https://doi.org/10.3390/molecules26092822.
[45] S. Liu, M. Bilal, K. Rizwan, I. Gul, T. Rasheed, H.M.N. Iqbal, Smart chemistry of enzyme immobilization using various support matrices – a review, Int. J. Biol. Macromol. 190 (2021) 396–408, https://doi.org/10.1016/j.ijbiomac.2021.09.006.
[46] O. Barbosa, C. Ortiz, Á. Berenguer-Murcia, R. Torres, R.C. Rodrigues, R. Fernandez-Lafuente, Strategies for the one-step immobilization-purification of enzymes as industrial biocatalysts, Biotechnol. Adv. 33 (2015) 435–456, https://doi.org/10.1016/j.biotechadv.2015.03.006.
[47] J.M. Bolivar, J.M. Woodley, R. Fernandez-Lafuente, Is enzyme immobilization a mature discipline? Some critical considerations to capitalize on the benefits of immobilization, Chem. Soc. Rev. (2022), https://doi.org/10.1039/D2CS00083K. In press.
[48] R.D. Schmid, R. Verger, Lipases: interfacial enzymes with attractive applications, Angew. Chem. Int. Ed. 37 (1998) 1608–1633, https://doi.org/10.1002/(SICI)1521-3773(19980703)37:12<1608::AID-ANIE1608>3.0.CO;2-V.
[49] R. Verger, 'Interfacial activation' of lipases: facts and artifacts, Trends Biotechnol. 15 (1997) 32–38, https://doi.org/10.1016/S0167-7799(96)10064-0.
[50] A.M. Brzozowski, U. Derewenda, Z.S. Derewenda, G.G. Dodson, D.M. Lawson, J. P. Turkenburg, F. Bjorkling, B. Huge-Jensen, S.A. Patkar, L. Thim, A model for interfacial activation in lipases from the structure of a fungal lipase-inhibitor complex, Nature 351 (1991) 491–494, https://doi.org/10.1038/351491a0.
[51] J. Yang, Y. Koga, H. Nakano, T. Yamane, Modifying the chain-length selectivity of the lipase from burkholderia cepacia KWI-56 through in vitro combinatorial mutagenesis in the substrate-binding site, Protein Eng. Des. Sel. 15 (2002) 147–152, https://doi.org/10.1093/protein/15.2.147.
[52] V.G. Tacias-Pascacio, S. Peirce, B. Torrestiana-Sanchez, M. Yates, A. Rosales-Quintero, J.J. Virgen-Ortíz, R. Fernandez-Lafuente, Evaluation of different commercial hydrophobic supports for the immobilization of lipases: tuning their stability, activity and specificity, RSC Adv. 6 (2016) 100281–100294, https://doi.org/10.1039/c6ra21730c.

[53] J. Van Buijtenen, B.A.C. Van As, M. Verbruggen, L. Roumen, J.A.J.M. Vekemans, K. Pieterse, P.A.J. Hilbers, L.A. Hulshof, A.R.A. Palmans, E.W. Meijer, Switching from S - to R- selectivity in the Candida antarctica lipase B-catalyzed ring-opening of ω-methylated lactones: tuning polymerizations by ring size, J. Am. Chem. Soc. 129 (2007) 7393–7398, https://doi.org/10.1021/ja071241a.
[54] S.S. Kumar, N. Arora, R. Bhatnagar, R. Gupta, Kinetic modulation of trichosporon asahii MSR 54 lipase in presence of organic solvents: altered fatty acid specificity and reversal of enantio selectivity during hydrolytic reactions, J. Mol. Catal. B Enzym. 59 (2009) 41–46, https://doi.org/10.1016/j.molcatb.2008.12.013.
[55] F. López-Gallego, O. Abian, J.M. Guisán, Altering the interfacial activation mechanism of a lipase by solid-phase selective chemical modification, Biochemistry 51 (2012) 7028–7036, https://doi.org/10.1021/bi300799v.
[56] M.D. Van Kampen, H.M. Verheij, M.R. Egmond, Modifying the substrate specificity of staphylococcal lipases, Biochemistry 38 (1999) 9524–9532, https://doi.org/10.1021/bi990096d.
[57] B. Zhang, P. Li, H. Zhang, H. Wang, X. Li, L. Tian, N. Ali, Z. Ali, Q. Zhang, Preparation of lipase/Zn3(PO4)2 hybrid nanoflower and its catalytic performance as an immobilized enzyme, Chem. Eng. J. 291 (2016) 287–297, https://doi.org/10.1016/j.cej.2016.01.104.
[58] J. Cui, Y. Zhao, R. Liu, C. Zhong, S. Jia, Surfactant-activated lipase hybrid nanoflowers with enhanced enzymatic performance, Sci. Rep. 6 (2016) 27928, https://doi.org/10.1038/srep27928.
[59] C. Ke, Y. Fan, Y. Chen, L. Xu, Y. Yan, A new lipase–inorganic hybrid nanoflower with enhanced enzyme activity, RSC Adv. 6 (2016) 19413–19416, https://doi.org/10.1039/C6RA01564F.
[60] C. Li, J. Zhao, Z. Zhang, Y. Jiang, M. Bilal, Y. Jiang, S. Jia, J. Cui, Self-assembly of activated lipase hybrid nanoflowers with superior activity and enhanced stability, Biochem. Eng. J. 158 (2020), 107582, https://doi.org/10.1016/j.bej.2020.107582.
[61] Y. Zhang, W. Sun, N.M. Elfeky, Y. Wang, D. Zhao, H. Zhou, J. Wang, Y. Bao, Self-assembly of lipase hybrid nanoflowers with bifunctional Ca2+ for improved activity and stability, Enzym. Microb. Technol. 132 (2020), 109408, https://doi.org/10.1016/j.enzmictec.2019.109408.
[62] Y. Du, J. Gao, W. Kong, L. Zhou, L. Ma, Y. He, Z. Huang, Y. Jiang, Enzymatic synthesis of glycerol carbonate using a immobilized on magnetic organosilica nanoflowers as a catalyst, ACS Omega 3 (2018) 6642–6650, https://doi.org/10.1021/acsomega.8b00746.
[63] W. Ren, Y. Li, J. Wang, L. Li, L. Xu, Y. Wu, Y. Wang, X. Fei, J. Tian, Synthesis of magnetic nanoflower immobilized lipase and its continuous catalytic application, New J. Chem. 43 (2019) 11082–11090, https://doi.org/10.1039/C8NJ06429F.
[64] K. Li, J. Wang, Y. He, M.A. Abdulrazaq, Y. Yan, Carbon nanotube-lipase hybrid nanoflowers with enhanced enzyme activity and enantioselectivity, J. Biotechnol. 281 (2018) 87–98, https://doi.org/10.1016/j.jbiotec.2018.06.344.
[65] L. Zhong, X. Jiao, H. Hu, X. Shen, J. Zhao, Y. Feng, C. Li, Y. Du, J. Cui, S. Jia, Activated magnetic lipase-inorganic hybrid nanoflowers: a highly active and recyclable nanobiocatalyst for biodiesel production, Renew. Energy 171 (2021) 825–832, https://doi.org/10.1016/j.renene.2021.02.155.
[66] H. Mohammadi-Mahani, A. Badoei-dalfard, Z. Karami, Synthesis and characterization of cross-linked lipase-metal hybrid nanoflowers on graphene oxide with increasing the enzymatic stability and reusability, Biochem. Eng. J. 172 (2021), 108038, https://doi.org/10.1016/j.bej.2021.108038.
[67] X. Luo, A.H. Mohammed Al-Antaki, A. Igder, K.A. Stubbs, P. Su, W. Zhang, G. A. Weiss, C.L. Raston, Vortex fluidic-mediated fabrication of fast gelated silica hydrogels with embedded laccase nanoflowers for real-time biosensing under flow, ACS Appl. Mater. Interfaces 12 (2020) 51999–52007, https://doi.org/10.1021/acsami.0c15669.
[68] M. Luo, M. Li, S. Jiang, H. Shao, J. Razal, D. Wang, J. Fang, Supported growth of inorganic-organic nanoflowers on 3D hierarchically porous nanofibrous membrane for enhanced enzymatic water treatment, J. Hazard. Mater. 381 (2020), 120947, https://doi.org/10.1016/j.jhazmat.2019.120947.
[69] T. Sun, M. Fu, J. Xing, Z. Ge, Magnetic nanoparticles encapsulated laccase nanoflowers: evaluation of enzymatic activity and reusability for degradation of malachite green, Water Sci. Technol. 81 (2020) 29–39, https://doi.org/10.2166/wst.2020.068.
[70] J.R. Guimarães, D. Carballares, J. Rocha-Martin, P.W. Tardioli, R. Fernandez-Lafuente, Stabilization of immobilized lipases by treatment with metallic phosphate salts, Int. J. Biol. Macromol. 213 (2022) 43–54, https://doi.org/10.1016/j.ijbiomac.2022.05.167.
[71] E.A. Manoel, J.C.S. dos Santos, D.M.G. Freire, N. Rueda, R. Fernandez-Lafuente, Immobilization of lipases on hydrophobic supports involves the open form of the enzyme, Enzym. Microb. Technol. 71 (2015) 53–57, https://doi.org/10.1016/j.enzmictec.2015.02.001.
[72] J.R. Guimarães, D. Carballares, P.W. Tardioli, J. Rocha-Martin, R. Fernandez-Lafuente, Tuning immobilized commercial lipase preparations features by simple treatment with metallic phosphate salts, Molecules 27 (2022) 4486, https://doi.org/10.3390/molecules27144486.
[73] R.C. Rodrigues, O. Barbosa, C. Ortiz, Á. Berenguer-Murcia, R. Torres, R. Fernandez-Lafuente, Amination of enzymes to improve biocatalyst performance: coupling genetic modification and physicochemical tools, RSC Adv. 4 (2014) 38350–38374, https://doi.org/10.1039/C4RA04625K.
[74] D. Carballares, J. Rocha-Martin, R. Fernandez-Lafuente, Preparation of a six-enzyme multilayer combi-biocatalyst: reuse of the most stable enzymes after inactivation of the least stable one, ACS Sustain. Chem. Eng. 10 (2022) 3920–3934, https://doi.org/10.1021/acssuschemeng.1c08180.
[75] O. Barbosa, M. Ruiz, C. Ortiz, M. Fernández, R. Torres, R. Fernandez-Lafuente, Modulation of the properties of immobilized CALB by chemical modification with 2,3,4-trinitrobenzenesulfonate or ethylendiamine. Advantages of using adsorbed lipases on hydrophobic supports, Process Biochem. 47 (2012) 867–876, https://doi.org/10.1016/j.procbio.2012.02.026.
[76] C. Garcia-Galan, J.C.S. dos Santos, O. Barbosa, R. Torres, E.B. Pereira, V. C. Corberan, L.R.B. Gonçalves, R. Fernandez-Lafuente, Tuning of lecitase features via solid-phase chemical modification: effect of the immobilization protocol, Process Biochem. 49 (2014) 604–616, https://doi.org/10.1016/j.procbio.2014.01.028.
[77] M. Ruiz, M. Galvis, O. Barbosa, C. Ortiz, R. Torres, R. Fernandez-Lafuente, Solid-phase modification with succinic polyethyleneglycol of aminated lipase B from Candida antarctica: effect of the immobilization protocol on enzyme catalytic properties, J. Mol. Catal. B Enzym. 87 (2013) 75–82, https://doi.org/10.1016/j.molcatb.2012.10.012.
[78] B.P. Carpenter, A.R. Talosig, J.T. Mulvey, J.G. Merham, J. Esquivel, B. Rose, A. F. Ogata, D.A. Fishman, J.P. Patterson, Role of molecular modification and protein folding in the nucleation and growth of protein–metal–organic frameworks, Chem. Mater. (2022), https://doi.org/10.1021/acs.chemmater.2c01903.
[79] R.C. Rodrigues, J.J. Virgen-Ortíz, J.C.S. dos Santos, Á. Berenguer-Murcia, A. R. Alcantara, O. Barbosa, C. Ortiz, R. Fernandez-Lafuente, Immobilization of lipases on hydrophobic supports: immobilization mechanism, advantages, problems, and solutions, Biotechnol. Adv. 37 (2019) 746–770, https://doi.org/10.1016/j.biotechadv.2019.04.003.
[80] O. Barbosa, C. Ortiz, Á. Berenguer-Murcia, R. Torres, R.C. Rodrigues, R. Fernandez-Lafuente, Glutaraldehyde in bio-catalysts design: a useful crosslinker and a versatile tool in enzyme immobilization, RSC Adv. 4 (2014) 1583–1600, https://doi.org/10.1039/C3RA45991H.
[81] L. Betancor, F. López-Gallego, A. Hidalgo, N. Alonso-Morales, G.D.-O.C. Mateo, R. Fernández-Lafuente, J.M. Guisán, Different mechanisms of protein immobilization on glutaraldehyde activated supports: effect of support activation and immobilization conditions, Enzym. Microb. Technol. 39 (2006) 877–882, https://doi.org/10.1016/j.enzmictec.2006.01.014.
[82] O. Barbosa, R. Torres, C. Ortiz, R. Fernandez-Lafuente, Versatility of glutaraldehyde to immobilize lipases: effect of the immobilization protocol on the properties of lipase B from Candida antarctica, Process Biochem. 47 (2012) 1220–1227, https://doi.org/10.1016/j.procbio.2012.04.019.
[83] S. Ait Braham, F. Hussain, R. Morellon-Sterling, S. Kamal, J.F. Kornecki, O. Barbosa, D.E. Kati, R. Fernandez-Lafuente, Cooperativity of covalent attachment and ion exchange on alcalase immobilization using glutaraldehyde chemistry: enzyme stabilization and improved proteolytic activity, Biotechnol. Prog. 35 (2019), e2768, https://doi.org/10.1002/btpr.2768.
[84] P.G. Vazquez-Ortega, M.T. Alcaraz-Fructuoso, J.A. Rojas-Contreras, J. López-Miranda, R. Fernandez-Lafuente, Stabilization of dimeric β-glucosidase from aspergillus Niger via glutaraldehyde immobilization under different conditions, Enzym. Microb. Technol. 110 (2018) 38–45, https://doi.org/10.1016/j.enzmictec.2017.12.007.
[85] T.L. de Albuquerque, S. Peirce, N. Rueda, A. Marzocchella, L.R.B. Gonçalves, M.V. P. Rocha, R. Fernandez-Lafuente, Ion exchange of β-galactosidase: the effect of the immobilization pH on enzyme stability, Process Biochem. 51 (2016) 875–880, https://doi.org/10.1016/j.procbio.2016.03.014.
[86] D. de Andrades, N.G. Graebin, M.K. Kadowaki, M.A.Z. Ayub, R. Fernandez-Lafuente, R.C. Rodrigues, Immobilization and stabilization of different β-glucosidases using the glutaraldehyde chemistry: optimal protocol depends on the enzyme, Int. J. Biol. Macromol. 129 (2019) 672–678, https://doi.org/10.1016/j.ijbiomac.2019.02.057.
[87] E.-H. Siar, S. Arana-Peña, O. Barbosa, M. Zidoune, R. Fernandez-Lafuente, Immobilization/stabilization of ficin extract on glutaraldehyde-activated agarose beads. Variables that control the final stability and activity in protein hydrolyses, Catalysts 8 (2018) 149, https://doi.org/10.3390/catal8040149.
[88] H. Zaak, S. Peirce, T. de Albuquerque, M. Sassi, R. Fernandez-Lafuente, Exploiting the versatility of aminated supports activated with glutaraldehyde to immobilize β-galactosidase from aspergillus oryzae 7 (2017) 250, https://doi.org/10.3390/catal7090250.
[89] L. Dal Magro, J.F. Kornecki, M.P. Klein, R.C. Rodrigues, R. Fernandez-Lafuente, Pectin lyase immobilization using the glutaraldehyde chemistry increases the enzyme operation range, Enzym. Microb. Technol. 132 (2020), 109397, https://doi.org/10.1016/j.enzmictec.2019.109397.
[90] T.L.D. Albuquerque, N. Rueda, J.C.S.Dos Santos, O. Barbosa, C. Ortiz, B. Binay, E. Özdemir, L.R.B. Gonçalves, R. Fernandez-Lafuente, Easy stabilization of interfacially activated lipases using heterofunctional divinyl sulfone activated-octyl agarose beads. Modulation of the immobilized enzymes by altering their nanoenvironment, Process Biochem. 51 (2016) 865–874.
[91] J.C.S. dos Santos, N. Rueda, O. Barbosa, J.F. Fernández-Sánchez, A.L. Medina-Castillo, T. Ramón-Márquez, M.C. Arias-Martos, M.C. Millán-Linares, J. Pedroche, M.del M. Yust, L.R.B. Gonçalves, R. Fernandez-Lafuente, Characterization of supports activated with divinyl sulfone as a tool to immobilize and stabilize enzymes via multipoint covalent attachment. Application to chymotrypsin, RSC Adv. 5 (2015) 20639–20649, https://doi.org/10.1039/C4RA16926C.
[92] J.C.S. dos Santos, N. Rueda, R. Torres, O. Barbosa, L.R.B. Gonçalves, R. Fernandez-Lafuente, Evaluation of divinylsulfone activated agarose to immobilize lipases and to tune their catalytic properties, Process Biochem. 50 (2015) 918–927, https://doi.org/10.1016/j.procbio.2015.03.018.
[93] J.C.S. dos Santos, N. Rueda, A. Sanchez, R. Villalonga, L.R.B. Gonçalves, R. Fernandez-Lafuente, Versatility of divinylsulfone supports permits the tuning of CALB properties during its immobilization, RSC Adv. 5 (2015) 35801–35810, https://doi.org/10.1039/C5RA03798K.

[94] J.C.S. dos Santos, N. Rueda, L.R.B. Gonçalves, R. Fernandez-Lafuente, Tuning the catalytic properties of lipases immobilized on divinylsulfone activated agarose by altering its nanoenvironment, Enzym. Microb. Technol. 77 (2015) 1–7, https://doi.org/10.1016/j.enzmictec.2015.05.001.
[95] J.C.S. dos Santos, N. Rueda, O. Barbosa, J. Pedroche, M. del Mar Yuste, L.R. B. Gonçalves, R. Fernandez-Lafuente, M.del C. Millán-Linares, Bovine trypsin immobilization on agarose activated with divinylsulfone: Improved activity and stability via multipoint covalent attachment, J. Mol. Catal. B Enzym. 117 (2015) 38–44, https://doi.org/10.1016/j.molcatb.2015.04.008.
[96] P.M.P. Souza, D. Carballares, N. Lopez-Carrobles, L.R.B. Gonçalves, F. Lopez-Gallego, S. Rodrigues, R. Fernandez-Lafuente, Enzyme-support interactions and inactivation conditions determine thermomyces lanuginosus lipase inactivation pathways: functional and florescence studies, Int. J. Biol. Macromol. 191 (2021) 79–91, https://doi.org/10.1016/j.ijbiomac.2021.09.061.
[97] A. Sanchez, J. Cruz, N. Rueda, J.C.S. dos Santos, R. Torres, C. Ortiz, R. Villalonga, R. Fernandez-Lafuente, Inactivation of immobilized trypsin under dissimilar conditions produces trypsin molecules with different structures, RSC Adv. 6 (2016) 27329–27334, https://doi.org/10.1039/C6RA03627A.
[98] R. Fernandez-Lafuente, Lipase from thermomyces lanuginosus: uses and prospects as an industrial biocatalyst, J. Mol. Catal. B Enzym. 62 (2010) 197–212, https://doi.org/10.1016/j.molcatb.2009.11.010.
[99] P. Domínguez De María, J.M. Sánchez-Montero, J.V. Sinisterra, A.R. Alcántara, Understanding Candida rugosa lipases: an overview, Biotechnol. Adv. 24 (2006) 180–196, https://doi.org/10.1016/j.biotechadv.2005.09.003.
[100] C.C. Akoh, G.-C. Lee, J.-F. Shaw, Protein engineering and applications of Candida rugosa lipase isoforms, Lipids 39 (2004) 513–526, https://doi.org/10.1007/s11745-004-1258-7.
[101] J. Barriuso, M.E. Vaquero, A. Prieto, M.J. Martínez, Structural traits and catalytic versatility of the lipases from the Candida rugosa-like family: a review, Biotechnol. Adv. 34 (2016) 874–885, https://doi.org/10.1016/j.biotechadv.2016.05.004.
[102] P. Dominguez de Maria, A. Alcantara, J. Carballeira, R. de la Casa, C. Garcia-Burgos, M. Hernaiz, J. Sanchez-Montero, J. Sinisterra, Candida rugosa lipase: a traditional and complex biocatalyst, Curr. Org. Chem. 10 (2006) 1053–1066, https://doi.org/10.2174/138527206777698057.
[103] M.M. Bradford, A rapid and sensitive method for the quantitation of microgram quantities of protein utilizing the principle of protein-dye binding, Anal. Biochem. 72 (1976) 248–254, https://doi.org/10.1016/0003-2697(76)90527-3.
[104] R. Fernandez-Lafuente, C.M. Rosell, V. Rodriguez, C. Santana, G. Soler, A. Bastida, J.M. Guisán, Preparation of activated supports containing low pK amino groups. A new tool for protein immobilization via the carboxyl coupling method, Enzym. Microb. Technol. 15 (1993) 546–550, https://doi.org/10.1016/0141-0229(93)90016-U.
[105] J. Boudrant, J.M. Woodley, R. Fernandez-Lafuente, Parameters necessary to define an immobilized enzyme preparation, Process Biochem. 90 (2020) 66–80, https://doi.org/10.1016/j.procbio.2019.11.026.
[106] D. Lombardo, O. Guy, Effect of alcohols on the hydrolysis catalyzed by human pancreatic carboxylic-ester hydrolase, Biochim. Biophys. Acta - Enzymol. 657 (1981) 425–437, https://doi.org/10.1016/0005-2744(81)90328-4.
[107] K. Hernandez, E. Garcia-Verdugo, R. Porcar, R. Fernandez-Lafuente, Hydrolysis of triacetin catalyzed by immobilized lipases: effect of the immobilization protocol and experimental conditions on diacetin yield, Enzym. Microb. Technol. 48 (2011) 510–517, https://doi.org/10.1016/j.enzmictec.2011.02.005.
[108] S. Arana-Peña, Y. Lokha, R. Fernández-Lafuente, Immobilization on octyl-agarose beads and some catalytic features of commercial preparations of lipase a from Candida antarctica (Novocor ADL): comparison with immobilized lipase B from Candida antarctica, Biotechnol. Prog. 35 (2019), e2735, https://doi.org/10.1002/btpr.2735.
[109] L. Wilson, J.M. Palomo, G. Fernández-Lorente, A. Illanes, J.M. Guisán, R. Fernández-Lafuente, Effect of lipase–lipase interactions in the activity, stability and specificity of a lipase from alcaligenes sp, Enzym. Microb. Technol. 39 (2006) 259–264, https://doi.org/10.1016/j.enzmictec.2005.10.015.
[110] J.M. Palomo, M. Fuentes, G. Fernández-Lorente, C. Mateo, J.M. Guisan, R. Fernández-Lafuente, General trend of lipase to self-assemble giving bimolecular aggregates greatly modifies the enzyme functionality, Biomacromolecules 4 (2003) 1–6, https://doi.org/10.1021/bm025729+.
[111] J.M. Palomo, C. Ortiz, G. Fernández-Lorente, M. Fuentes, J.M. Guisán, R. Fernández-Lafuente, Lipase-lipase interactions as a new tool to immobilize and modulate the lipase properties, Enzym. Microb. Technol. 36 (2005) 447–454, https://doi.org/10.1016/j.enzmictec.2004.09.013.
[112] J.M. Palomo, C. Ortiz, M. Fuentes, G. Fernandez-Lorente, J.M. Guisan, R. Fernandez-Lafuente, Use of immobilized lipases for lipase purification via specific lipase-lipase interactions, J. Chromatogr. A 1038 (2004) 267–273, https://doi.org/10.1016/j.chroma.2004.03.058.
[113] O. Abian, V. Grazú, J. Hermoso, R. González, J.L. García, R. Fernández-Lafuente, J.M. Guisán, Stabilization of penicillin G acylase from Escherichia coli: site-directed mutagenesis of the protein surface to increase multipoint covalent attachment, Appl. Environ. Microbiol. 70 (2004) 1249–1251, https://doi.org/10.1128/AEM.70.2.1249-1251.2004.
[114] J. Mansfeld, G. Vriend, B. Van den Burg, V.G.H. Eijsink, R. Ulbrich-Hofmann, Probing the unfolding region in a thermolysin-like protease by site-specific immobilization, Biochemistry 38 (1999) 8240–8245, https://doi.org/10.1021/bi990008p.
[115] J. Mansfeld, R. Ulbrich-Hofmann, Site-specific and random immobilization of thermolysin-like proteases reflected in the thermal inactivation kinetics, Biotechnol. Appl. Biochem. 32 (2000) 189, https://doi.org/10.1042/BA20000059.
[116] R.C. Rodrigues, C. Ortiz, Á. Berenguer-Murcia, R. Torres, R. Fernández-Lafuente, Modifying enzyme activity and selectivity by immobilization, Chem. Soc. Rev. 42 (2013) 6290–6307, https://doi.org/10.1039/c2cs35231a.
[117] J.M. Bolivar, B. Nidetzky, On the relationship between structure and catalytic effectiveness in solid surface-immobilized enzymes: advances in methodology and the quest for a single-molecule perspective, Biochim. Biophys. Acta - Proteins Proteomics 1868 (2020), 140333, https://doi.org/10.1016/j.bbapap.2019.140333.
[118] J.M. Bolivar, I. Eisl, B. Nidetzky, Advanced characterization of immobilized enzymes as heterogeneous biocatalysts, Catal. Today 259 (2016) 66–80, https://doi.org/10.1016/j.cattod.2015.05.004.
[119] W. Guo, X. Zou, H. Jiang, K.J. Koebke, M. Hoarau, R. Crisci, T. Lu, T. Wei, E.N. G. Marsh, Z. Chen, Molecular structure of the surface-immobilized super uranyl binding protein, J. Phys. Chem. B 125 (2021) 7706–7716, https://doi.org/10.1021/acs.jpcb.1c03849.
[120] X. Zou, S. Wei, S. Badieyan, M. Schroeder, J. Jasensky, C.L. Brooks, E.N.G. Marsh, Z. Chen, Investigating the effect of two-point surface attachment on enzyme stability and activity, J. Am. Chem. Soc. 140 (2018) 16560–16569, https://doi.org/10.1021/jacs.8b08138.
[121] J. Jasensky, K. Ferguson, M. Baria, X. Zou, R. McGinnis, A. Kaneshiro, S. Badieyan, S. Wei, E.N.G. Marsh, Z. Chen, Simultaneous observation of the orientation and activity of surface-immobilized enzymes, Langmuir 34 (2018) 9133–9140, https://doi.org/10.1021/acs.langmuir.8b01657.
[122] Y. Li, T.L. Ogorzalek, S. Wei, X. Zhang, P. Yang, J. Jasensky, C.L. Brooks, E.N. G. Marsh, Z. Chen, Effect of immobilization site on the orientation and activity of surface-tethered enzymes, Phys. Chem. Chem. Phys. 20 (2018) 1021–1029, https://doi.org/10.1039/C7CP06063G.
[123] S. Badieyan, Q. Wang, X. Zou, Y. Li, M. Herron, N.L. Abbott, Z. Chen, E.N. G. Marsh, Engineered surface-immobilized enzyme that retains high levels of catalytic activity in air, J. Am. Chem. Soc. 139 (2017) 2872–2875, https://doi.org/10.1021/jacs.6b12174.
[124] T.L. Ogorzalek, S. Wei, Y. Liu, Q. Wang, C.L. Brooks, Z. Chen, E.N.G. Marsh, Molecular-level insights into orientation-dependent changes in the thermal stability of enzymes covalently immobilized on surfaces, Langmuir 31 (2015) 6145–6153, https://doi.org/10.1021/acs.langmuir.5b01735.
[125] N.R. Mohamad, N.H.C. Marzuki, N.A. Buang, F. Huyop, R.A. Wahab, An overview of technologies for immobilization of enzymes and surface analysis techniques for immobilized enzymes, Biotechnol. Biotechnol. Equip. 29 (2015) 205–220, https://doi.org/10.1080/13102818.2015.1008192.
[126] N. Carlsson, H. Gustafsson, C. Thörn, L. Olsson, K. Holmberg, B. Åkerman, Enzymes immobilized in mesoporous silica: a physical–chemical perspective, Adv. Colloid Interf. Sci. 205 (2014) 339–360, https://doi.org/10.1016/j.cis.2013.08.010.